Energy & Buildings 359 (2026) 117289

Contents lists available at ScienceDirect

Energy & Buildings

journal homepage: www.elsevier.com/locate/enb

District-scale life cycle costing of climate-neutral retrofits, based on automatic envelope detection workflows and LOD3 3D city model

Anthony Robert Suppa [a,*], Marta Carla Bottero [a], Vincenzo Corrado [b], Federico Dell'Anna [a]

[a] Interuniversity Department of Regional and Urban Studies and Planning (DIST), Politecnico di Torino, Viale Mattioli 39, 10125 Turin, TO Italy
[b] Department of Energy, Politecnico di Torino, Corso Duca degli Abruzzi 24, 10129 Turin, Italy

ARTICLE INFO

Keywords:
Life cycle costing
Urban building energy modeling (UBEM)
Advanced urban sensing
Artificial intelligence
Retrofit scenario analysis
Level of detail (LOD)

ABSTRACT

Policymakers guiding the decarbonization transition must make decisions around energy and CO_2 reductions that are linked to financial expenditures. This study supports decision-making in the buildings sector by combining urban building energy modeling and life cycle costing (LCC) for district-scale retrofit scenarios. The LCC is completed at level of detail (LOD) 3, enriched with exterior wall, roof, and window areas extracted from advanced urban sensing and artificial intelligence techniques. In a case district of 1,291 residential buildings in Turin, Italy, detected envelope quantities are applied to unit costs, resulting in investment costs of €13,723 to €27,272 per dwelling, significantly higher than budgeted for the EU mission 100 Climate-Neutral Cities. A total of 80 scenarios are modeled, including 10 retrofit packages under two scenarios for roof renovation (with and without occupied attics), and with four deployment scenarios to modulate retrofit rates and emission factors in the electricity supply. The research shows complex outcomes under different deployment scenarios, though packages combining envelope retrofits with high-temperature heat pumps consistently result in the greatest emission reductions and lowest cumulative discounted cash flow (CDCF) per quantity of CO_2 saved. For six packages, accelerating retrofit deployment led to 1%-18% lower CDCF, as energy savings offset investment costs over 30 years, even though a gross floor area of 1.4 million m^2 is retrofitted, compared to 855,000 m^2 under slower deployment scenarios. The value of the work is to prove the use of automatic detection techniques in urban-scale LCC, and to provide decision support tools to policymakers guiding the rapid transition to climate neutrality.

1. Introduction

High investment costs and scarce financial resources challenge a rapid transition to net-zero CO_2 emissions. Globally, spending on decarbonization is estimated at $275 trillion by 2050, averaging $9.2 trillion annually[1]. Preceding the Paris Agreement's 2050 net-zero deadline, the EU mission "100 Climate-Neutral Cities by 2030" aims to eliminate territorial emissions within each participating city (or a district thereof), at a cost of €96 billion, or €10,000 per citizen[2]. A priority for EU decarbonization is the buildings sector, accounting for 40% of energy use and 36% of energy-related emissions in the region[3].

Informing EU policy in the buildings sector is the Energy Performance of Buildings Directive (EPBD) [4], calling for member states to use financial incentives to promote retrofitting, balancing investment cost and energy savings throughout the building life cycle. The EPBD also promotes district-scale retrofits, leading to quicker and less costly decarbonization of the building stock. Another key policy, the Renovation Wave, aims to double retrofit rates to 2% per year and foster deep retrofits following the "efficiency first" principle, to renovate 35 million buildings by 2030[3].

Two research fields supporting the energy transition are life cycle costing (LCC) and urban building energy modeling (UBEM). Firstly, LCC determines costs and savings of retrofits, including investment costs, operational costs, and end-of-life costs. Discounting future cash flows to present values and summing these over the life cycle provides an equal basis for comparison among scenarios. Secondly, UBEM uses computational tools to calculate energy use in baseline and retrofit conditions for clusters of buildings at district or city scale, accounting for dynamics of individual buildings, inter-building effects, and microclimate[5,6]. Among UBEM studies simulating retrofits, 40% of these analyzed not only energy but also financial implications, quantifying investment costs

* Corresponding author.
E-mail addresses: anthony.suppa@polito.it (A.R. Suppa), marta.bottero@polito.it (M.C. Bottero), vincenzo.corrado@polito.it (V. Corrado), federico.dellanna@polito.it (F. Dell'Anna).

https://doi.org/10.1016/j.enbuild.2026.117289
Received 29 July 2025; Received in revised form 4 February 2026; Accepted 8 March 2026
Available online 12 March 2026
0378-7788/© 2026 The Author(s). Published by Elsevier B.V. This is an open access article under the CC BY-NC-ND license (http://creativecommons.org/licenses/by-nc-nd/4.0/).

Nomenclature

Abbreviations

AI	artificial intelligence
COM	cost-optimal methodology
COP	coefficient of performance
DHW	domestic hot water
EF	emission factor
EPBD	energy performance of buildings directive
FC	fan coil
GC	global cost
GIS	geographic information systems
GSV	Google Street View
HP	heat pump
LCC	life cycle costing
LiDAR	light detection and ranging
LOD	level of detail
NPV	net present value
RB	reference building
SVI	street view imagery
UBEM	urban building energy model / modeling
WWR	window-to-wall ratio

Retrofit codes & deployment scenarios

E	envelope
M	mechanical
PV	photovoltaic
nZEB	nearly zero-energy building standard
PH	Passive House standard
EXT	exterior of roof insulation
INT	interior of roof insulation
HT	high-temperature heat pump
LT	low-temperature heat pump
RW	Renovation Wave scenario
100CNC	100 Climate-Neutral Cities scenario

LCC nomenclature

CO_a	annual operating costs
CO_{init}	initial investment costs
CO_{fin}	final decommissioning cost
D_f	discount rate
RAT	price development rate
t_0	starting year
t_{TC}	calculation period
VAL_{fin}	residual value

and/or energy savings, most frequently on a non-discounted basis[7]. Our literature review (Section 2) shows that few LCC studies use UBEM, and few UBEM studies calculate LCC.

Urban-scale LCC and UBEM commonly use bottom-up modeling. In UBEM, one begins by quantifying energy use at the individual building level, often based on building archetypes, then accumulating results to represent the district or city[8,9]. Our literature review shows most urban-scale LCC studies also begin with reference buildings, calculate investment cost for each, then upscale based on geometry from GIS or floor areas in statistical databases (e.g. [10–12]). Besides geometry, UBEM requires parameters of building height, envelope construction details, occupancy schedules, and many others; since publicly available data are often lacking, extensive default data and assumptions are used [6]. Indeed, missing data in UBEM studies are significant barriers to model effectiveness and add uncertainty and error into building energy estimates[9,13]. The literature also notes that UBEM could take advantage of advanced urban sensing and artificial intelligence (AI) techniques to fill data gaps for construction types, energy systems, and window-to-wall ratio (WWR)[14].

In UBEM, level of detail (LOD) and accuracy of the 3D city model are essential, with fundamental parameters calculated from the geometry, such as surface areas, conditioned space, and relation between buildings, including whether buildings are adjoining[15]. In 3D city modeling, LOD denotes a model's adherence to real-world conditions and has implications for its usability[16]. As Fig. 1 indicates, increasing LOD levels include: (0) a building footprint; (1) an extruded shoebox; (2) added pitched roof; (3) added overhangs, shades, glazing; and (4) added full interior layout and features [6,16]. LOD appears frequently in UBEM literature[8,9,17], and LOD1 is noted as most common[15]. The LOD concept is largely absent from urban-scale LCC literature, other than two recent LCC studies in Munich that created an LOD2 model[18,19].

In this work, we apply advanced urban sensing and AI techniques to calculate investment costs for LCC. The method begins by extracting roof areas from LiDAR data and WWR from street view imagery (SVI). These are incorporated into an LOD3 3D city model, where exterior walls are also separated from shared party walls of adjoining buildings. Extracted envelope areas equate to quantities of added insulation or window substitution, and applying unit costs provides investment costs for the LCC, also at LOD3. The UBEM calculates energy use in baseline and retrofit conditions, informing energy costs. The UBEM can be considered at LOD 1+, since it simplifies building geometries with flat roofs, and adds the automatically extracted WWRs to each building façade. Finally, the LCC determines cumulative discounted cash flow and savings for energy and CO_2 emissions in 10 retrofit packages, under two scenarios for roof renovation (with and without occupied attics), plus four deployment scenarios, for a total of 80 scenarios modeled. Deployment scenarios include renovation rates per the EU's Renovation Wave policy and the 100 Climate-Neutral Cities by 2030 mission.

The research is structured as follows. Section 2 reviews urban-scale LCC literature. Section 3 details the methodology. Section 4 describes the case study, a district in Turin, Italy, with 1,291 residential buildings. Section 5 presents the results, including validation of roof geometry calculations; post-retrofit energy and emissions savings; global cost from the LCC model; and LCC under the deployment scenarios. Sections 6 and 7 provide a discussion and conclusion.

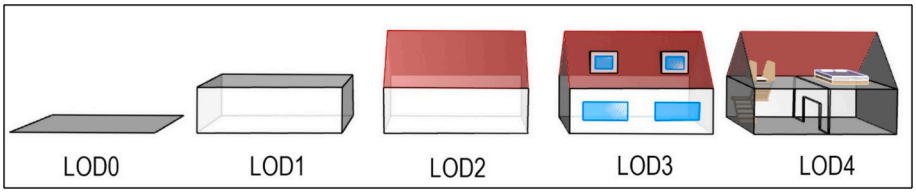


Fig. 1. Level of detail (LOD) to represent buildings in 3D city modeling. and Source: authors' elaboration following [6,16].

2. Literature review

In recent years, several works have conducted life cycle costing for urban-scale retrofit scenarios, as summarized in Table 1. Of the 14 studies reviewed, most calculate "global cost" (GC) according to EN 15459-1[20] or following EU cost-optimal methodology (COM) regulations[21,22]. The GC approach tallies a series of costs – investment, energy, maintenance, replacement, decommissioning, and CO_2 emission costs – as well as residual value, discounting these to the initial year when investments are made and adding the result. Around one-third of the reviewed studies only report investment and energy costs, and most do not calculate CO_2 or decommissioning costs. Analysis periods of 30–50 years are typical, reflecting life spans of major building components.

While both COM and net present value (NPV) approaches calculate GC, COM calculates the cost-optimal level of an energy reduction over the life cycle, while NPV calculates total discounted cash flow for evaluated scenarios. One of the studies included costs/savings outside the economic domain, using a cost-benefit analysis to value social and environmental domains, including health benefits, green job creation, and emissions avoided[25].

All reviewed studies used unit prices to determine investment costs, expressed as cost per square meter for envelope components and cost per unit or per kW for mechanical and renewable energy systems. Government price lists, private engineering/consulting company reports, scientific literature, and utility company data informed unit prices in the studies.

Applying costs per square meter to envelope elements, such as wall insulation or windows to be replaced, requires geometries or quantities of each element. To calculate geometries, most studies begin with archetype or reference buildings (RBs), which have typical parameters defined according to technical reports such as TABULA in Italy[32], scientific literature defining archetypes in Northern Spain[33], or other local databases in Sweden[12]. RBs can then be upscaled to the entire study area using GIS data, as observed in nine of the studies, or using floor areas from statistical databases.

Similarly, most of the reviewed studies quantify energy use and savings at the building level based on RBs, before upscaling to the district level. Such an approach uses either calculations under steady-state conditions with monthly/annual time resolution, or simplified dynamic or full dynamic simulations with hourly/sub-hourly resolution.

Only three of the reviewed studies can be considered UBEMs. Two are physics-based UBEMs, conducting separate simplified dynamic energy simulations for each building in the district[28,30]. The third is a hybrid UBEM, using energy signatures from measured consumption data to create district-specific building archetypes, then performing one building-level simulation per archetype[31]. In a recent review of retrofit-focused UBEM studies[7], only two reviewed studies conducted LCC on district-scale retrofits[30,31], while seven others completed financial analysis using annual energy savings or simple payback period, which are metrics based on a single point in time.

Thus, a gap is evident in the literature, as few LCC-focused studies quantify urban energy use and savings based on simulation individual buildings, and most UBEM-focused studies do not quantify life cycle costs.

Additional literature gaps are related to LOD for envelope modeling. LOD in urban-scale geometry calculations was not clear in all reviewed studies except two with an LOD2 model[18,19]. Thus, only two studies accounted for roof geometry on a building-by-building basis according to roof types (such as flat, gable, or hip roofs). Regarding exterior walls, one can theoretically multiply building heights by footprints in GIS to derive wall areas, though the studies did not address adjoining buildings with party walls, where exterior insulation would not be added during retrofitting. Another issue with adjoining buildings, it is not clear whether or how studies exclude costs for windows on shared party walls. Regarding glazing, studies might have window surface areas in each RB (e.g. [12]) or window area based on a percentage of the floor area (e.g. [11]) and apply these values to each building of the same archetype based on total floor areas in GIS. None of the reviewed studies used distinct glazing ratios particular to each building. Uncertainty around quantities of envelope retrofits introduces error in cost calculations, with potentially large variations in quantities of walls and roofs to be insulated or windows to be substituted.

To address the gaps in the literature, the present work provides automatic detection workflows to augment the level of detail in the GIS database. Roofs are classified using LiDAR data, and roof geometries are automatically generated in the LOD3 3D city model. For walls, a tool in the LOD3 model distinguishes exterior and shared party walls. For windows, distinct WWRs for each building face are detected using deep learning, and these ratios are applied to the LOD3 model. All buildings are modeled in a full-dynamic UBEM with sub-hourly time resolution, accounting for actual geometry and individualized roof and window parameters, thus informing an LCC with energy consumption and savings.

3. Methodology

Per Fig. 2, the methodology includes: (1) GIS data preparation and roof classification; (2) calculation of WWR using deep learning and SVI; (3) creation of a LOD3 city model; (4) urban building energy simulation; and (5) life cycle costing. Each is detailed in the following sub-sections.

3.1. GIS data preparation and roof classification

The workflow requires GIS data containing building geometry, metadata (building height and stories), and complete LiDAR point cloud coverage, obtained from a municipal GIS database. Roof classification based on LiDAR data is conducted using the existing toolset "3D Buildings Solution" within ArcGIS Pro[34,35], leading to one of three roof type classifications, including flat, gable, and hip roofs (see Fig. 3). A series of surface raster files are built from the LiDAR points, which are used to classify roof types as follows: flat roof if more than 45% of the surface is flat; otherwise, gable roof if there are 1–2 unique plane aspects, and hip roof if there are 3 or more plane aspects [35]. The classification uses minimum building heights of 2.4 m and minimum roof areas of 7 m^2 for sloped roofs and 23 m^2 for flat roofs, so that objects such as street posts or vehicles are not classified as roofs [36]. Finally, all GIS data are exported to SHP files for use in the 3D city model.

3.2. Window detection using deep learning

Glazing ratios are obtained using deep-learning-based detections in our previous work[37]. The workflow uses GIS coordinates to extract and stitch façade images from Google Street View (GSV), then trains and validates a YOLOv9 model[38] to detect WWR. This deep learning architecture was selected based on previous successes with YOLO-based models in façade parsing, including Kong and Fan [39] and Sezen et al. [40]. The workflow included annotating 576 out of 2,393 images extracted from GSV, training and validating the YOLOv9 model over 92 epochs, running inference mode to detect bounding boxes for glazing objects, walls, and garages, and finally converting to WWR based on pixel areas. Façade WWR predictions showed to be within ± 5% of ground truth WWRs for 92% of images, with examples depicted in Fig. 4. The workflow builds on precedent façade parsing works using a custom algorithm to automatically classify non-street-facing sides and rears and estimate WWR at these non-visible building faces, resulting in a distinct WWR for each face of each building. Façade WWRs are multiplied by line segment length and building height to estimate window areas, informing window substitution costs in the LCC. All details from the window detection stage, including deep learning hyperparameters, evaluation metrics, and the classification algorithm steps and validation are described in Suppa et al. [37].

Table 1
Precedent literature. Energy analysis: C = calculations; MD = measured data; BEM = building-scale energy model; UBEM = urban building energy model; SS = steady-state; SD = simplified dynamic; FD = full dynamic. Financial analysis: NPV = net present value; COM = cost-optimal methodology; CBA = cost-benefit analysis. Quantity calculation: RB = reference building; EPC = energy performance certificates; SI = site investigation. Unit costs: G = government report; U = utility company; P = private company report; L = scientific literature. Costs in LCC: I = investment; E = energy; M = maintenance; Rep = replacement; Res = residual; CO_2 = CO_2 emission costs; D = decommissioning.

Reference	Case study		Methods			Cost sources		Financial model rates		Costs included in LCC						
	Location	Scope & size (buildings)	Energy analysis	Financial analysis	Quantity calculation	Invest-ment	Energy	Inflation	Discount	I	E	M	Rep	Res	CO_2	D
[10]	Naples, Italy	Social housing multi-family (4)	BEM-FD	COM	RB, GIS	L	L	–	4%	√	√	√	√	–	–	–
[23]	Gonen, Turkey	Residential multi-family (56)	C-SS	COM	SI	–	U	5.08%	3.97%	√	√	–	–	–	–	–
[24]	Braga, Portugal	Social housing single-family (50)	BEM-FD	COM	SI, national database	P	–	–	3%	√	√	√	√	√	–	√
[25]	Turin, Italy	Residential multi-family (22)	C-SS	CBA	RB	G	U	–	5%	√	√	√	√	√	√	–
[11]	Turin, Italy	Residential buildings (5,585)	C-SS	COM	RB, GIS	G	–	2%	3.5%	√	√	√	√	√	–	–
[26]	Bari, Italy	Social housing multi-family (1,800)	C-SS	NPV	RB, GIS	–	–	–	4%	√	√	–	–	–	–	–
[27]	Bilbao, Spain	Residential buildings (98,259)	BEM-FD	COM	RB, national statistics	P, G	G	1.7%	1.7% & 4% scenarios	√	√	√	√	√	√	–
[28]	Bolzano, Italy	Residential buildings (95)	UBEM-SD	NPV	RB, GIS	L	U	–	3%	√	√	–	–	–	–	–
[18] and [19]	Munich, Germany	Residential buildings (115,305 and 196)	C-SS	NPV	RB, GIS	P	–	Energy: 5% Investment: 2%	–	√	√	–	√	–	√	–
[12]	Visby, Sweden	Historic residential buildings (920)	–	COM	RB, GIS, municipal database	P	U	–	5%	√	√	–	–	–	–	–
[29]	Italy	Office building stock (64,911)	BEM-FD	NPV	RB, national database	G, L	L	–	3%	√	√	–	–	–	–	–
[30]	Gothenburg, Sweden	Residential multi-family (5,901)	UBEM-SD	NPV	RB, GIS, EPC	L, G	L, P	Energy: 0.37%, 0.44% & 0.47% scenarios	4%	√	√	√	√	–	–	–
[31]	Stockholm, Sweden	Residential multi-family (5,400)	MD for all bldgs, one BEM-FD for each RB	NPV	RB, GIS	P	P	–	4%, 8% & 20% scenarios	√	√	–	–	–	–	–

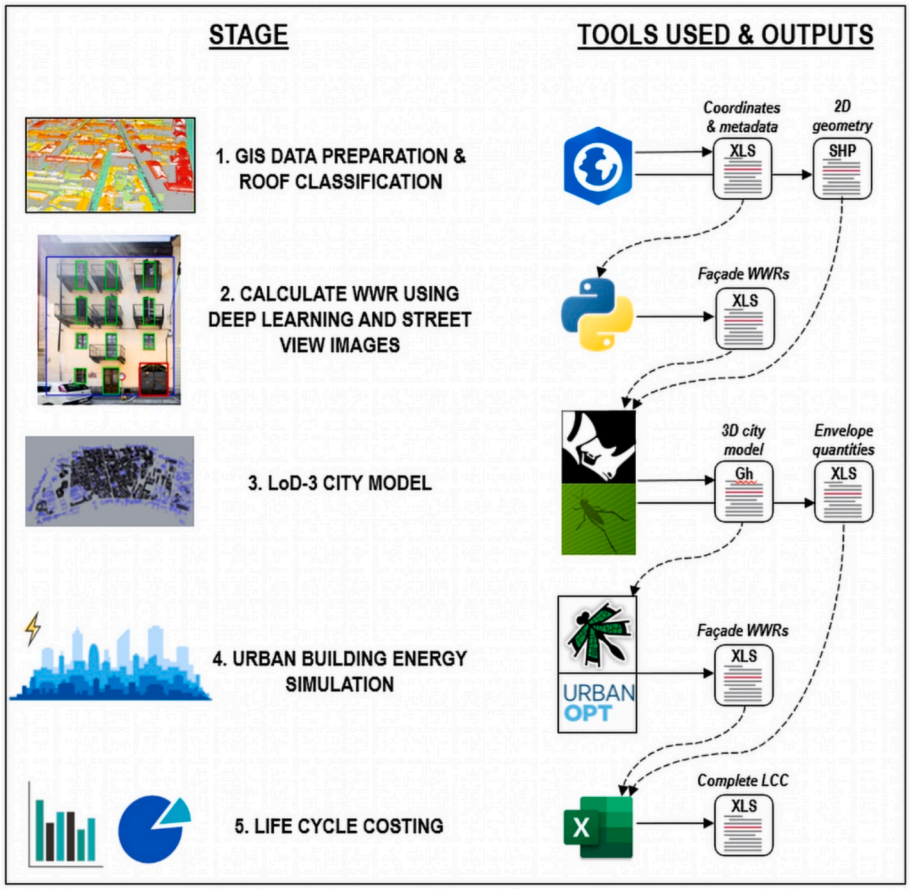


Fig. 2. Methodology overview.
Source: authors' elaboration using icons from Fotor.com and referenced software.

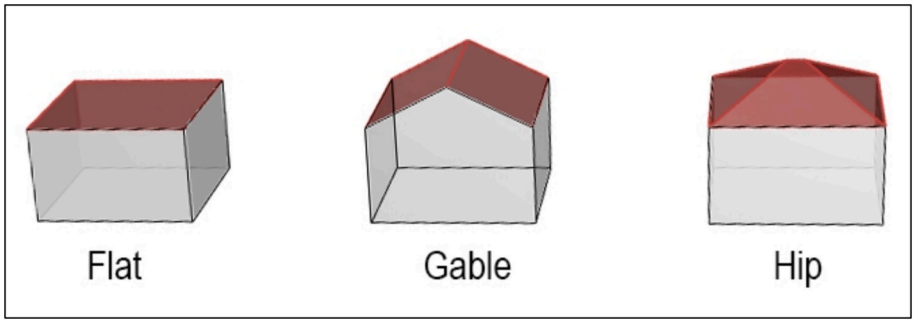


Fig. 3. Flat, gable, and hip roof types classified using GIS workflow.
Source: authors' elaboration following [35].

3.3. LOD3 3D city model

The LOD3 3D city model provides automatic area calculations for roofs and exterior walls, which are used for retrofit cost calculations. Inputs include one SHP file per archetype (there are 24 archetypes present in the case study of Section 4), with building footprints and metadata including number of stories, building height, roof classifications, and roof heights from GIS, plus WWR values from the deep-learning workflow. The files are imported into Grasshopper, the graphical algorithm editor within Rhino software[41], where the plug-ins Honeybee and Dragonfly [42], designed for building- and urban-scale energy modeling, further develop the model.

To model roofs, a custom Grasshopper script[1] segments footprints into those with four or more than four vertices. The latter are L-shapes or complex building shapes, for which we estimate a roof ridge using the Dragonfly tool "straight skeleton", producing a tree-branch-like polyline within each footprint. This tool follows the algorithm of Felkel & Obrdrzalek [43] and is intended to create thermal zones for energy models, though we observe that the central portion of the straight skeleton approximates a building's roof ridgeline. Accordingly, our

[1] The script is made available at: https://github.com/asuptor/AutoRoofGeometry



Fig. 4. Detections from the deep learning model with windows (green), wall (blue), and garage door (red). Differences in WWR between detections and ground truth are + 0.1% (left), +3.7% (center), and –6.6% (right). (For interpretation of the references to colour in this figure legend, the reader is referred to the web version of this article.)
Source: images are facsimiles of original SVI, using photos taken by authors.

script isolates the central polyline by detecting line segments connected to the building footprint, as depicted in Fig. 5. For hip roofs, the ridge polyline is transposed upward using the eaves-to-peak height from GIS. For gable roofs, the process is nearly identical, though we first extend the approximated ridge to the building outline before transposing upward.

For complex building shapes, we use the "patch surface" tool with the footprint polygon and roof ridge polyline, approximating the roof in a single curved surface. For buildings with four vertices, each roof surface is constructed directly using the "4-point surface" tool. The key output is roof area, to be used for investment cost calculation in the LCC.

Post-processing is required for gable roofs, subtracting the triangle at short ends of buildings, which are exterior walls to be insulated and not pitched roofs. For gable roofs with four vertices, the end wall areas are computed in Grasshopper, as shown in Fig. 5. For gable roofs with more than four vertices, the end wall areas are subtracted in a Python script based on GIS data.

To calculate error in the automatic roof area workflow, we sample 140 roofs in the dataset and use Rhino to trace roof lines on top of aerial orthophotos. The 2D lines are extruded to 3D roof shapes using the eaves-to-peak heights from LiDAR data, with error recorded for each.

For walls in the 3D model, one must distinguish exterior walls from party walls in adjoining buildings, as only the former require insulation. Accordingly, we repurpose another Dragonfly tool called "process alleys", designed to remove glazing from walls in a narrow alley condition by sensing distance between a wall and nearby buildings. We use a distance condition of nearly zero (0.05 m in case of errors in the GIS file) and set sensed walls to an adiabatic boundary condition, which is the correct condition for adjoining walls in a UBEM[44,45]. A Dragonfly tool provides a summary of walls by boundary condition, so that only exterior wall areas are calculated and applied to insulation costs in the LCC. A visualization of the result is depicted in Fig. 6.

The completed LOD3 3D city model thus calculates envelope quantities for the LCC, and once parametrized, forms the basis for the UBEM, as detailed below.

3.4. Urban building energy model

The UBEM is also developed within Rhino/Grasshopper and uses a digital building library to parameterize walls, floors, roofs, and windows with building material thickness, density, and conductivity. Also parameterized are schedules for occupancy, lighting, domestic hot water (DHW), and heating/cooling, and the creation of libraries and schedules follows our previous research[46].

The baseline digital building library contains construction assemblies where materials and *U*-values approximate existing conditions, based on local building archetypes. In the case study (see Section 4), TABULA defines target *U*-values, which are executed using assemblies from Italian technical report UNI/TR 11552 [47], adjusting material thicknesses as required. Two libraries for envelope retrofits are programmed, as per Table 2, firstly according to "nearly zero-energy building" (nZEB) standards (Italian [48], and secondly, per Passive House (PH) standards[49].

Once parameterized, the UBEM computes energy need for heating, cooling, and DHW, and energy use for lighting and electrical equipment. The UBEM also models shading objects, including all structures within a 50-meter buffer of simulated buildings. A Dragonfly tool runs the

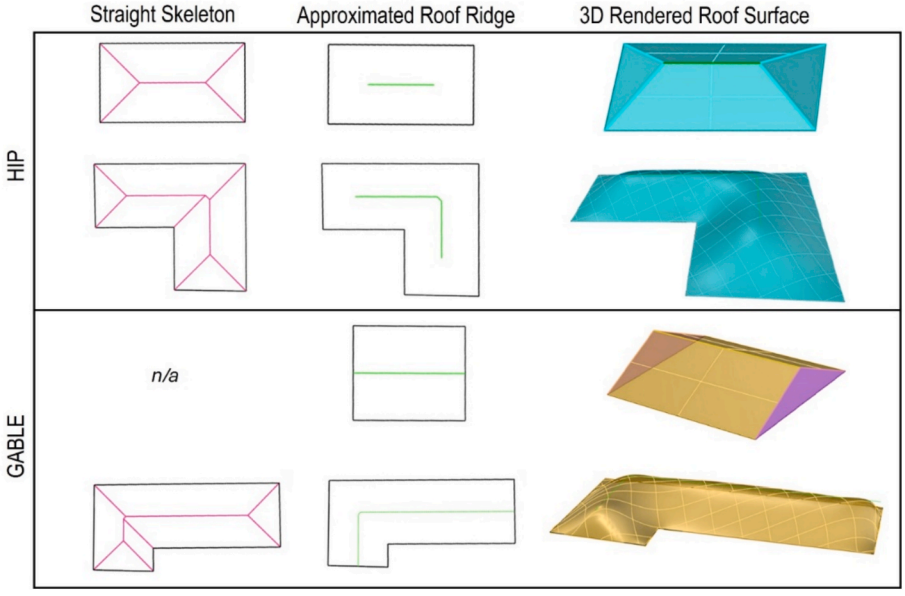


Fig. 5. Building footprints with straight skeletons, approximated roof ridges, and resulting roof surfaces. In the gable roofs with four-vertex footprints, the triangle shapes (purple) are allocated to exterior wall quantities, as these are to be covered in wall insulation. (For interpretation of the references to colour in this figure legend, the reader is referred to the web version of this article.)
Source: authors' elaboration.

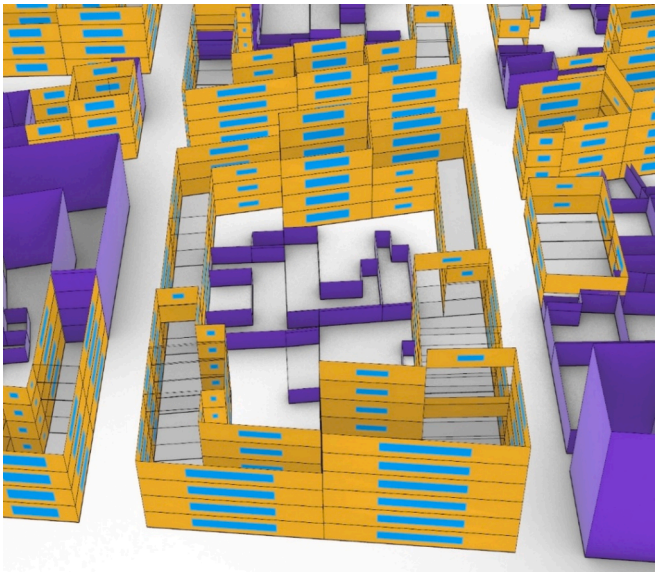


Fig. 6. Visualization of 3D city model with roofs removed to reveal party walls between adjoining buildings, shown as transparent. In purple are structures not simulated for energy but acting as shading objects. (For interpretation of the references to colour in this figure legend, the reader is referred to the web version of this article.)
Source: authors' elaboration.

Table 2
Energy-related parameters for retrofits modeled. Sources: (1) [48], for climate zone "E"; (2) [49]; (3) [50]; (4) [51]. * denotes that PH requires SHGC of 0.50, though 0.35 is used to match the nZEB value.

Retrofit package	Description	Energy Model Values	
Envelope	Roof insulation	**nZEB** (1) $U = 0.22$ W/(m^{2}K)	**PH** (2) $U = 0.15$ W/(m^{2}K)
	Ground floor insulation	$U = 0.26$ W/(m^{2}K)	$U = 0.15$ W/(m^{2}K)
	Wall insulation	$U = 0.26$ W/(m^{2}K)	$U = 0.15$ W/(m^{2}K)
	Window replacement	$U = 1.40$ W/(m^{2}K) SHGC = 0.35	$U = 0.80$ W/(m^{2}K) SHGC = 0.35*
Mechanical	High-temperature space heating	COP = 2.5 (1)	
	DHW heating	COP = 2.5 (1)	
	Low-temperature space heating	COP = 3.0 (1)	
	DHW heating	COP = 2.5 (1)	
	Space cooling	COP = 2.5 (1)	
		Maximum power of fan coils = 20 W	
PV	1. Roof-mounted monocrystalline PV panels	1. Panel efficiency = 16% (3)	
	2. PV-integrated roof tiles, for historic buildings	2. Panel efficiency = 13.57% (4)	
		All PV: performance ratio = 84% (3)	

URBANopt module [52] to conduct dynamic simulations on a floor-by-floor basis for each building in the district, in 15-minute timesteps using EnergyPlus [53], in parallel using separate CPUs.

To convert energy need to energy use values for heating, cooling, and DHW, we post-process the simulation results by dividing by the generation efficiencies of existing gas or oil boilers from TABULA, ranging 0.71 to 0.98 depending on the archetype, or COP values noted in Table 2 in the case of mechanical retrofits. We add values for losses due to distribution, control, emission, and storage, as well as auxiliary energy (e.g. pumps), also according to TABULA.

To model rooftop PV energy generation, we use the "raster solar radiation" tool within ArcGIS Pro, based on a digital surface model, plus slope and aspect rasters, all created from LiDAR data. Upon simulation, results are filtered to include only roofs with annual insolation exceeding 1,000 kWh/m^2 and minimum roof size of 40 m^2[50], and to exclude slopes steeper than 45 degrees and north-facing slopes (i.e., aspects between 22.5 and 337.5 degrees). The PV simulation results in average energy generated per roof (in kWh/m^2•year) and the area (in m^2) that meets the imposed criteria. For standard roof-mount PV panels, roof areas are further multiplied by reduction coefficients of 0.9 for pitched and 0.8 for flat roofs, as well as panel spacing coefficient of 0.9 for pitched and 0.46 for flat roofs [50]. Reduction coefficients are not applied to the historic buildings, which receive PV-integrated roof tiles for the entire suitable roof surface.

Results for energy use and PV generation are then incorporated into the LCC, as detailed next.

3.5. Life cycle costing

This section describes GC calculations, investment cost estimation, the retrofit packages, and the deployment scenarios modeled.

3.5.1. Global cost

The LCC method is based on EN 15459:2017 [20] to calculate GC over 30 years, according to the formula:

$$GC = CO_{init} + \sum_{j}\left[\sum_{i=1}^{TC}\left(CO_{a(i)}(j)^{*}\left(1 + RAT_{(i)}(j)\right) - VAL_{fin(TC)}(j)\right)^{*}D_{f(i)}\right] \quad (1)$$

where:
CO_{init} are initial investment costs;
TC is the calculation period;
$CO_{a(i)}(j)$ are annual costs for year i for component j;
$RAT_{(i)}(j)$ is the price development for year i, i.e. the inflation rate, for each component j;
$D_{f(i)}$ is the discount factor for year i;
$VAL_{fin(TC)}(j)$ is the residual value of component j at the end of the calculation period, discounted to value at the starting year.

Annual costs include maintenance and energy costs, as well as periodic replacement costs. Since CO_2 emission costs are embedded in energy prices under the EU emissions trading scheme, this study does not separately calculate CO_2 costs, to avoid double-counting. Also excluded are decommissioning costs.

Energy prices of 0.3864 €/kWh for electricity and 0.1136 €/kWh for natural gas are taken from the Italian national energy regulator and include taxes and levies[54]. Sale of PV energy is based on the current minimum guaranteed price of 0.0463 €/kWh[55]. Maintenance costs range 0%-6% of initial investment costs, and component life spans range 15–40 years, as detailed in Appendix Table A1, so that components are replaced if they reach end of life within the 30-year analysis period.

An annual inflation rate of 2% is used for all costs beyond the first year, based on the European Central Bank's long-term target rate[56]. As for discount rate, most precedents reviewed in Section 2 use rates of 3–4%, and here we select 4%. We select the higher end of the range since mortgage rates have increased in recent years—while previously in the 1%-2% range until early 2022, they have risen to 3.3% at present [57]—which increases homeowners' weighted average cost of capital, thus putting upward pressure on discount rates. As life cycle costs are sensitive to discount rates and energy inflation rates[29,58,59], we conduct a sensitivity analysis to show the effect of these rates on GC.

3.5.2. Investment cost estimation

To calculate investment costs, the LOD3 city model provides surface areas of exterior walls, roofs/ceilings, floors, and windows. Retrofits of these components follow the construction technologies in Table 3, with

Table 3
LCC-related parameters for retrofits modeled. Retrofit codes: E = envelope; M = mechanical; PV = photovoltaics; INT = interior of attic; EXT = exterior of roof; HT = high temperature; LT = low temperature. Sources: (1) [60]; (2) [51]; (3) [61]; (4) [50].

Retrofit code	Description	Construction technology	Insulation nZEB	Insulation PH	Unit costs nZEB (1)	Unit costs PH (1)	Quantity / sizing
E_INT	Ceiling insulation (within attic space)	Mineral fiber insulation, sprayed into unheated attic.	10–19 cm	16–29 cm	20–24 €/m^2	24–32 €/m^2	Building footprint area.
E_EXT	Roof insulation (from exterior)	1. Sloped: includes removal and replacement of roof tiles and battens to add exterior insulation.	1. 12–16 cm	1. 20–26 cm	1. 205–217 €/m^2	1. 205–217 €/m^2	From LOD 3D city model: 3D roof surface areas.
		2. Flat: includes installation of new flat roofing membrane atop new exterior insulation.	2. 12–16 cm	2. 20–26 cm	2. 126–138 €/m^2	2. 126–138 €/m^2	
E_INT & E_EXT	Ground floor insulation	Foil-faced mineral wool insulation pinned to underside of ground floor within unheated cellar.	4–12 cm	14–22 cm	20–40 €/m^2	44–63 €/m^2	Building footprint area.
E_INT & E_EXT	Wall insulation	1. *Eras 2–3:* interior EPS insulation laminated with gypsum board panels. Include interior stucco, plus allowance for electrical relocations and trim carpentry repairs.	1. 10–12 cm	1. 20–22 cm	1. 49–55 €/m^2	1. 81–88 €/m^2	From LOD 3D city model: adjoining party walls automatically subtracted from total wall area.
		2. *Eras 4–8:* exterior mineral wool insulation & exterior stucco.	2. 3–12 cm	2. 14–22 cm	2. 96–122 €/m^2	2. 128–150 €/m^2	
E_INT & E_EXT	Window replacement	1. *Eras 2–3:* wood-framed casement windows with spectrally selective low-e coating.	Double glazing	Triple glazing	1. 585 €/m^2	1. 716 €/m^2	From window detection workflow: WWR multiplied by wall area.
		2. *Eras 4–8:* PVC-framed tilt-and-turn windows with spectrally-selective low-e coating.			2. 461 €/m^2	2. 570 €/m^2	
M_HT	HT space heating DHW heating	Air-to-water HP for combined space heating and DHW heating. Distribution via radiators in existing buildings.	–		HP: 5,059 € (6 kW) to 89,805 € (397 kW) (2)		Heating/cooling load sizing from energy model, plus power to yield day's supply of DHW within 6 h.
M_LT	LT space heating DHW heating Space cooling	Air-to-water HP for combined space cooling, space heating, and DHW heating. Distribution via new FCs.	–		HP: same as above FC: 563 € each (2)		HP: same as above FC: 5 per AB & MF building; 3 per floor in SF & TH building. (3)
PV	1. PV-integrated roof tiles	1. *Eras 2–3:* PV-integrated roof tiles installed during roof removal & replacement, including inverter.	–		1. 6,378 to 7,070 €/kW (2)		From LOD 3D city model: 3D roof surface areas, then multiplied by noted reduction coefficients from (4). PV array size multiplied by efficiency to determine peak power (kW).
	2. Standard roof-mount monocrystal PV panels	2. *Eras 4–8:* standard PV panels installed on existing roof, including inverter.			2. 1,577 to 2,280 €/kW (2)		

insulation thicknesses calculated individually for each building archetype. Calculated areas are multiplied by unit prices, which can be found in governmental or private company reports, such as price lists from Region of Piedmont [60] and Region of Veneto [60] for the case study. The unit prices are for the complete system to be installed, given existing conditions. For example, for exterior roof insulation, the work includes removal and replacement of existing roof tiles, battens, and waterproofing membrane.

We calculate costs to complete the full scope of work. For example, envelope retrofits require scaffolding for access and protection, and waste must be transported from the construction site and disposed. Some mechanical retrofits carry additional costs, such as conversion from autonomous to centralized systems, as described in the following sub-section and itemized in Appendix Table A2.

3.5.3. Retrofit packages

For building envelopes, our modeling includes three variations, related to: (i) historic building status, (ii) whether attics are occupied, and (iii) retrofit standards.

Buildings with historic status must avoid extensive exterior alterations, and thus wall insulation is conducted from the inside and window substitutions match existing wood-framed windows, with a cost premium of 25% on the latter. For interior-side insulation, there is a cost savings of 36%-55% compared to exterior insulation, but the insulation and wallboard consume space within residences.[2] To avoid losing interior space, all non-historic buildings are modeled with exterior insulation. Additionally, PV panels atop historic roofs are avoided. Instead, we model installation of PV-integrated roof tiles, which have been used in historic retrofit projects including at UNESCO World Heritage site Pompeii[62]. These also carry a significant premium, around 3–4 times costlier than standard PV.

Second, we include envelope scenarios for two roof insulation methods, as it may not be known whether building attics are unoccupied or are renovated with inhabitable units. In the former (INT), insulation can be easily sprayed from the attic interior onto the attic floor, using cellulose or mineral fiber, thus insulating the upper unit ceiling from the unheated attic. In the latter (EXT), for sloped roofs, roof tiles and battens must be removed and reinstalled from the exterior with new insulation and waterproofing membrane. Flat roofs are similar, requiring removal and reinstallation of exterior membrane (but not battens) to add insulation. The uncertainty has significant cost impact, with costs per m^2 at 7 to 10 times greater for exterior roofing methods compared to interior

[2] For the case study, 1% to 2% of interior space are lost in the average 60 m^2 dwelling unit.

attic insulation.

Third, all envelope retrofit packages are modeled to nZEB standards and to Passive House (PH) standards, as detailed in Section 3.4.

For mechanical retrofits, we consider two scenarios, one with high-temperature (HT) space heating and a second at low temperature (LT). In the former, the existing hydronic radiators within dwellings are maintained, while centralized gas or oil boilers are swapped with high-temperature air-to-water HPs. Maintaining radiators saves on investment cost, and similarly, we assume that existing piping can be maintained in existing centralized systems. Where archetypes note that systems are autonomous, we estimate costs to convert these systems to centralized as per Appendix Table A2.

In the LT scenario, existing radiators are substituted for fan coils, carrying costs of fan coils, wiring, and condensate piping. Fan coils make the system capable of space cooling, a significant benefit considering a warming climate. We assume that space cooling and DHW can be provided in summer using the same HP, thus adding costs for motorized valves, pumps, and chilled buffer tanks to facilitate the dual function of the system.

Retrofit packages are applied cumulatively, beginning with the envelope measures, then adding mechanical measures, and finally adding renewable energy with PV, in line with the "efficiency-first" principle of the EPBD [4]. Thus, we first evaluate two envelope packages, according to nZEB and PH standards. Adding the two mechanical systems (HT and LT) in combination with each envelope package leads to a further four packages. Next, adding PV to each of the latter adds another four packages. The 10 resulting packages are modeled with INT and EXT roof insulation scenarios, for a total of 20 retrofit packages evaluated for life cycle cost and CO_2 emissions.

3.5.4. Retrofit deployment scenarios

While GC analysis allows comparison of retrofit packages to the baseline condition, it instantly implements retrofits in a fictitious "year 0". To better represent reality, we model several deployment scenarios, first at a 2% renovation rate following the EU Renovation Wave policy, and second at a 20% rate to meet Turin's commitment to the EU mission 100 Climate-Neutral Cities by 2030. For these scenarios, we measure conversion of electricity to carbon dioxide at a constant rate—currently 303 g/kWh[63]—and at a variable rate where the electricity supply reduces CO_2 content by 12.1 g/kWh each year until 2050 to meet EU decarbonization targets.

The deployment scenarios also model Italian "Ecobonus" and "Bonus Ristrutturazioni" incentives for years 2026 and later, rebating 36% of global energy retrofit costs to a maximum of €100,000 per dwelling, and 36% of photovoltaic costs with limits of €96,000 and 20 kW installed capacity per dwelling. Homeowners must pay for retrofits up front and receive tax rebates equally distributed over the 10 subsequent years [64].

4. Case study

The methodology is applied to a case district in Turin, Italy, known as *Circoscrizione 6* (District 6), which is home to 104,408 residents [65] and thus meets the minimum population for 100 Climate-Neutral Cities. Building geometry, metadata, LiDAR data, and aerial orthophotos are from the municipal GIS database[66], showing the district to contain 5,964 buildings, of which 3,925 are residential. Only residential buildings are considered in the present research, since the archetype-based energy modelling approach relies on TABULA, which includes only residential buildings. Buildings are only included in the case study if WWR was successfully extracted in our previous research[37], totaling 1,291 residential buildings. In that work, a successful extraction was defined as having one or more façade images extracted from GSV, façade WWRs estimated with deep learning, and non-visible building sides and rears estimated using our automatic classification algorithm. Furthermore, the work only included buildings meeting a footprint squareness tolerance, to avoid upscaling WWR for the entire building in long, rectangular buildings if WWR was extracted only one short side. Thus the 1,291 buildings extracted in our previous work represent the case study in this work, with 1.4 million m^2 of gross floor area (GFA) and an estimated 20,100 dwelling units. The buildings can be subdivided into 1,432 volumes; for example, a building may contain a 2-story and a 6-story volume, and the UBEM simulates these separately to ensure accurate story count and building heights.

To parameterize buildings with envelope assemblies and mechanical systems, we use archetypes from the Italian implementation of the European TABULA project[32]. TABULA classifies buildings as single-family (SF), terraced house (TH), multi-family (MF), and apartment block (AB) types, which are subcategorized by construction era. The eras are as follows: 1 & 2 – before 1918; 3 – 1919 to 1945; 4 – 1946 to 1960; 5 – 1961 to 1970; 6 – 1971 to 1990; 7 – 1991 to 2005; 8 – 2006 and after. TABULA eras 1 and 2 are combined in this work because the GIS data relies on Italian national statistics agency eras that do not distinguish between buildings built before 1918.

The district buildings were previously classified into TABULA archetypes in Suppa & Corrado [46], based on surface/volume ratios, story count, and footprint area using GIS data. Classified buildings are coded accordingly; for example, residential ("R") buildings of type AB and era 3 are coded "R3AB". Based on GFA, 78% of the buildings in the case study are type AB, 17% are MF, 2% are SF, and 4% are TH. Six archetypes represent 85% of the case study GFA, including R3AB, R3MF, R4AB, R4MF, R5AB, and R6AB. TABULA notes that buildings of eras 2–5 contain no insulation, and those of era 6 contain only low levels of insulation. Thus, the case represents an opportunity to demonstrate significant energy savings through retrofitting. Furthermore, district heating is not available in this part of the city, making the case study ideal to evaluate efficiency gains when switching from combustion-based heating to heat pumps.

Regarding retrofit details for the case study, buildings built up to 1945 (era 2 and 3) have a greater probability of historic status, and thus historic-appropriate measures noted in Section 3.5.3 are adopted. TABULA assumes that all AB and MF archetypes (95% of district GFA) have unoccupied attics, yet it is readily observable that some of these buildings have occupied attics, and there is no data quantifying the number of occupied versus unoccupied in the GIS database. Thus, the two roof retrofit methods (INT and EXT) per Section 3.5.3 are modeled. Finally, TABULA indicates that archetypes R65MF, R6MF, and R7AB have autonomous heating systems, and AB and MF types of eras 4, 6, 7, 8, plus archetype R5MF have autonomous DHW systems. Thus, costs of conversion from autonomous to centralized systems per Appendix Table A2 are calculated in the LCC.

5. Results

5.1. Roof geometry

To check accuracy of the roof surface calculation workflow, 140 roofs were manually measured using 2D polylines traced in Rhino on top of orthophotos, then extruded to 3D using eaves-to-peak heights from LiDAR, as depicted in Fig. 7.

Overall, −10.4% error was observed, considering the manually measured roof areas as true, as detailed in Table 4. The GIS classification algorithm was more effective in classifying gable roofs than hip roofs, with 55 of 70 and 34 of 70 correctly classified, respectively. Notably, 23% of the sampled roofs had one gable and one hip end, which is not an option for the existing ArcGIS classifier to detect, though detectoin error was not linked to the accuracy of the classifier. There was a correlation between number of building footprint vertices and percent error, with buildings with four vertices showing −11.2% and −12.7% error, while those with greater than four vertices showed −9.6% and −9.1% error. There was also a correlation between percent error and building type, where buildings attached on two sides had the lowest error (−9.2%),



Fig. 7. Roof measurement with gable (orange), hip (cyan), and one gable end/one hip end (purple). (For interpretation of the references to colour in this figure legend, the reader is referred to the web version of this article.)
Source: authors' elaboration on top of municipal orthophotos [66].

followed by buildings attached on one side (−10.3%), and finally detached buildings (−10.9%).

5.2. Energy and CO_2 savings

Depicting primary energy use in baseline and retrofit conditions is Fig. 8, for the six most prevalent archetypes (representing 85% of district GFA) and the overall district. Factors of 1.05 and 2.42 are used to convert site energy to primary energy for natural gas and grid electricity, respectively[67]. The retrofit package with Passive House envelope standards plus mechanical retrofits with high-temperature HPs leads to the greatest energy savings of −58% in the overall district. The overall results show energy savings of 48%-53% for envelope-only packages, and 52%-58% savings when mechanical retrofits are added.

PV packages are not included in the figure since they do not affect energy use, but rather substitute grid energy with renewable on-site energy, thereby reducing CO_2 emissions. Fig. 9 shows how site energy and CO_2 emissions decrease with the cumulative addition of envelope, mechanical, and PV retrofits. Gas remains the principal energy carrier for space heating and DHW in the baseline and two envelope-only packages, while all other packages eliminate site combustion by electrifying heat production via HPs. The addition of PV reduces emissions in the district by 6% compared to the envelope plus mechanical packages, resulting in CO_2 reductions of 74%-78% from baseline. Conversion factors are 212 and 303 gCO_2/kWh for natural gas and grid electricity, respectively[63]. Since the energy model simplifies geometries using only flat roofs, the energy results do not distinguish between INT and EXT scenarios.

5.3. Global cost

Investment costs were calculated for all retrofit packages with interior and exterior roof scenarios, as summarized in Table 5. Costs ranged from €13,723 to €27,272 per dwelling. The cost premium to compete roof retrofits from the exterior in the case of occupied attics ranged from €3,157 to €3,414 per dwelling, or €64 to €69 million for the district.

GC was calculated for baseline and retrofit packages, as depicted in Fig. 10, using a 4% discount rate. The figure shows, firstly, costs without incentives and, secondly, investment costs less government incentives, namely the homeowner's perspective. Here, for a fair comparison, the costs are limited to investment and energy costs, since maintenance, replacement, and residual costs are difficult to calculate for existing buildings in the baseline condition. Without incentives, six of the 10 packages showed lower GC compared to baseline for the INT scenarios, saving 4%-17% compared to baseline GC. The higher cost of EXT roof retrofits meant that only three of these packages had lower GC compared to baseline, with reduced savings of 2%-11%. When government incentives are applied, these reduce the homeowner's investment costs significantly, and all packages have a lower GC than baseline, with 1%-25% savings.

5.4. LCC with deployment scenarios

Retrofit deployment was modeled according to the EU Renovation Wave scenario (RW) and EU mission 100 Climate-Neutral Cities scenario (100CNC), with retrofit rates of 2% and 20% respectively. Results maintaining the emission factor (EF) in the current electricity supply are summarized in Table 6, indicating the cumulative discounted cash flow (CDCF) over the analysis period and the carbon emission reduction from baseline after 30 years. Consistent with the GC analysis, the envelope-only package to nZEB standards (E_nZEB) showed the lowest CDCF in all scenarios. The table also indicates CDCF required to reduce each percentage of baseline CO_2, essentially a measure of cost efficiency to effect decarbonization. The packages featuring high-temperature heat pumps and PV have the lowest total CDCF per CO_2 reduction, in all constant EF scenarios, with similar CDCF per CO_2 reduction for envelope retrofits to nZEB and PH standards (E_nZEB & M_HT & PV and E_PH & M_HT & PV).

Table 7 indicates the same metrics but with variable EF, shifting to zero CO_2 in the electricity supply on a straight-line basis by 2050. CDCF values are the same in both scenarios, and are not repeated. From constant to variable EF scenarios, the incremental CO_2 savings in envelope-only packages are minor, but are significant when mechanical packages are added, as fossil-fuel boilers are converted to HPs running on decarbonized electricity. In the Renovation Wave scenario, the reduction for all packages with HPs is 69% from baseline, since 61% of the most energy-intensive building stock is retrofitted by 2050. With accelerated retrofit rates in the 100CNC scenario, all buildings are retrofitted, and those with mechanical retrofits all produce zero emissions. Furthermore, the package with lowest CDCF per CO_2 savings shifts, as all scenarios with HPs have the same emissions but different investment costs, and the package with envelope retrofits to nZEB standards with high-temperature HPs and without PV (E_nZEB & M_HT) becomes the most cost-efficient.

Table 4
Results of manual measurement of roof areas compared to automatically calculated areas. Building type: D = detached, A1 = attached on one side, A2 = attached on two sides. * percent error = (detected – true) / true.

Building footprint vertices	GIS classification	Count	Actual roof type			Roof area (m^2)		Percent error*	Building type		
			All sides gable	All sides hip	One side hip, one side gable	Manual measurement *(true)*	Automatic calculation *(detected)*		D	A1	A2
4	Gable	35	29	2	4	6,983	6,201	−11.2%	13	10	12
>4	Gable	35	26	3	6	10,389	9,396	−9.6%	14	10	11
4	Hip	35	0	25	10	8,694	7,593	−12.7%	25	10	0
>4	Hip	35	14	9	12	13,348	12,128	−9.1%	9	21	5
Overall		140	69	39	32	39,414	35,318	−10.4%	61	51	28

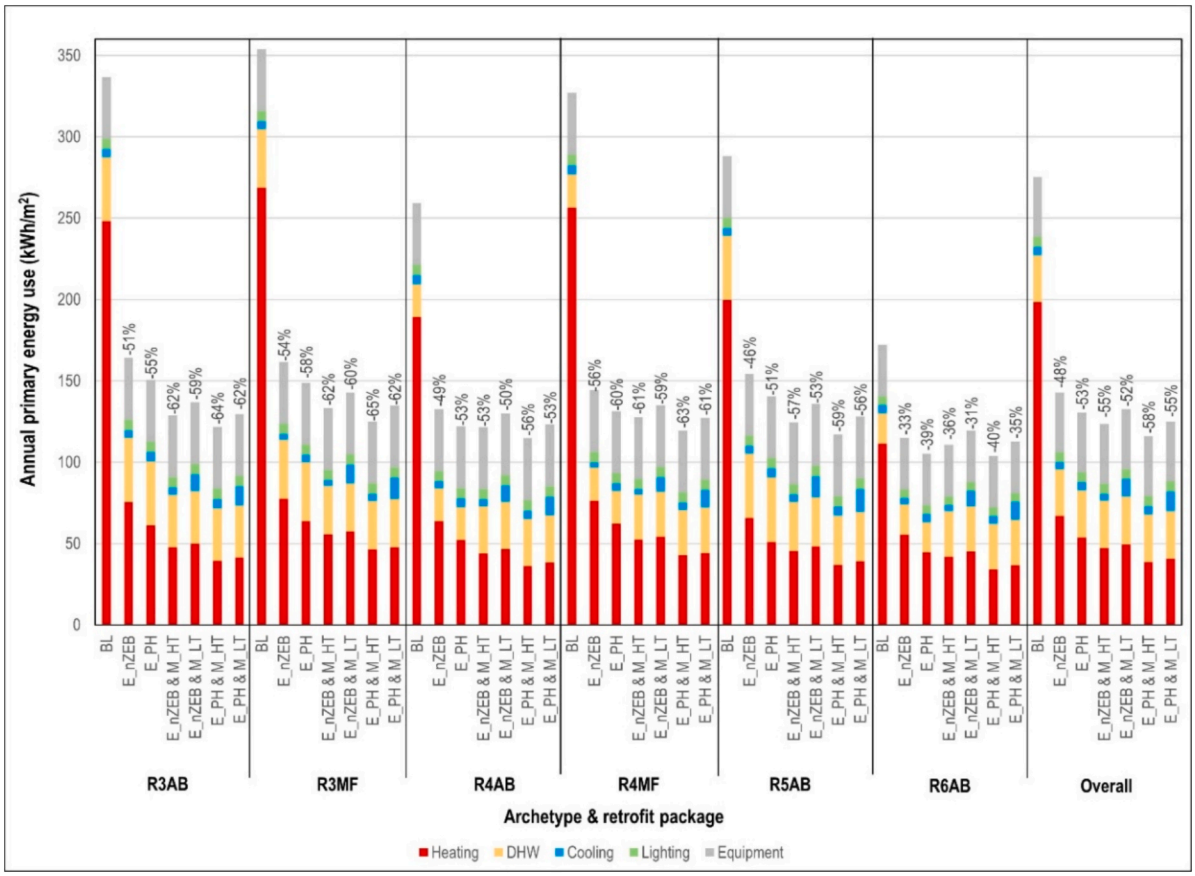


Fig. 8. Primary energy use, by energy service, in the overall district and six most prevalent archetypes. BL = baseline; E_nZEB / E_PH = envelope retrofits to nZEB or Passive House standards; M_HT / M_LT = mechanical retrofits with high-temperature or low-temperature heat pumps.
Source: authors' elaboration.

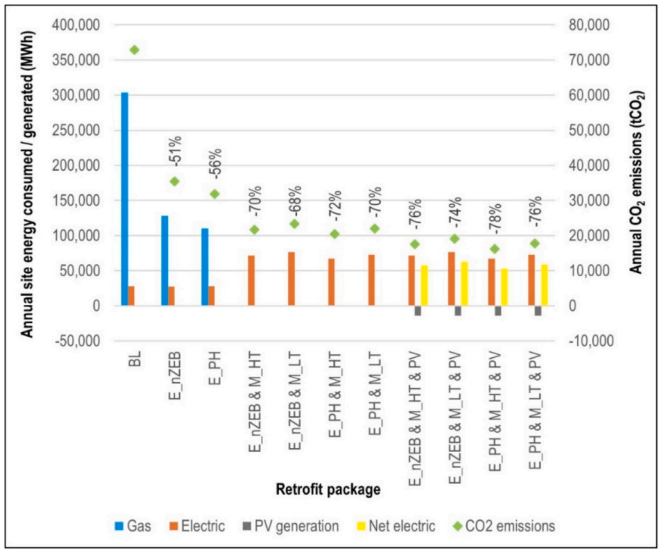


Fig. 9. Annual site energy consumed/generated and annual CO_2 emissions, by retrofit package, for the overall case study. Percentages indicate CO_2 emission reductions from baseline. BL = baseline; E_nZEB / E_PH = envelope retrofits to nZEB or Passive House standards; M_HT / M_LT = mechanical retrofits with high-temperature or low-temperature heat pumps; PV = rooftop photovoltaics added to building.
Source: authors' elaboration.

Decomposing CDCF into energy, investment, maintenance, and replacement costs provides additional insight, as depicted in Figs. 11 and 12 for four selected EXT packages for RW and 100CNC scenarios, both under variable EF. The INT scenarios (not depicted) reveal identical trends, but with lower investment costs. Energy cost remains the most significant factor under RW, accounting for 63%-79% of CDCF. With more of the building stock retrofitted under 100CNC, energy cost shrinks to 32%-49% of CDCF. Total investment costs (private plus government) increase from 20% to 32% of CDCF under RW, to 44%-61% of CDCF under 100CNC. Combined maintenance and replacement costs range 1%-6% of CDCF under RW and 2%-17% of CDCF under 100CNC, with all packages containing low-temperature HPs (M_LT) at the upper end of the ranges.

These shifting percentages have impacts on overall CDCF in the two scenarios. For all packages other than those with low-temperature HPs, overall CDCF was lower under 100CNC compared to RW, even though all buildings are retrofitted in the former scenario, with 1%-18% lower CDCF, depending on retrofit package. This is due to retrofits conducted earlier, resulting in lower energy expenditures over the 30-year analysis. The higher combined investment, maintenance, and replacement costs associated with the low-temperature HPs meant that these packages had higher CDCF under 100CNC compared to RW.

6. Discussion

This section begins with a discussion of the energy simulation, including validation and limitations of the results and future perspectives. Second is a sensitivity analysis to increase the robustness of the results. Last is a discussion of the envelope detection workflows (Section 6.3) and for the combined cost, energy, and emissions results (Section 6.4), discussing the significance of the results, validity, limitations, and

Table 5
Investment costs calculated for each retrofit package, under INT and EXT roof scenarios.

Retrofit package	_INT Total cost for district (million €)	Cost per GFA (€/m²)	Cost per dwelling (€/unit)	_EXT Total cost for district (million €)	Cost per GFA (€/m²)	Cost per dwelling (€/unit)
E_nZEB	275.8	196	13,723	339.3	242	16,880
E_PH	335.6	239	16,694	404.2	288	20,108
E_nZEB & M_HT	308.0	219	15,322	371.4	265	18,479
E_nZEB & M_LT	391.7	279	19,486	455.1	324	22,643
E_PH & M_HT	365.4	260	18,179	434.0	309	21,593
E_PH & M_LT	449.1	320	22,342	517.7	369	25,757
E_nZEB & M_HT & PV	338.4	241	16,837	401.9	286	19,994
E_nZEB & M_LT & PV	422.1	301	21,001	485.6	346	24,158
E_PH & M_HT & PV	395.8	282	19,694	464.5	331	23,108
E_PH & M_LT & PV	479.5	342	23,857	548.2	390	27,272

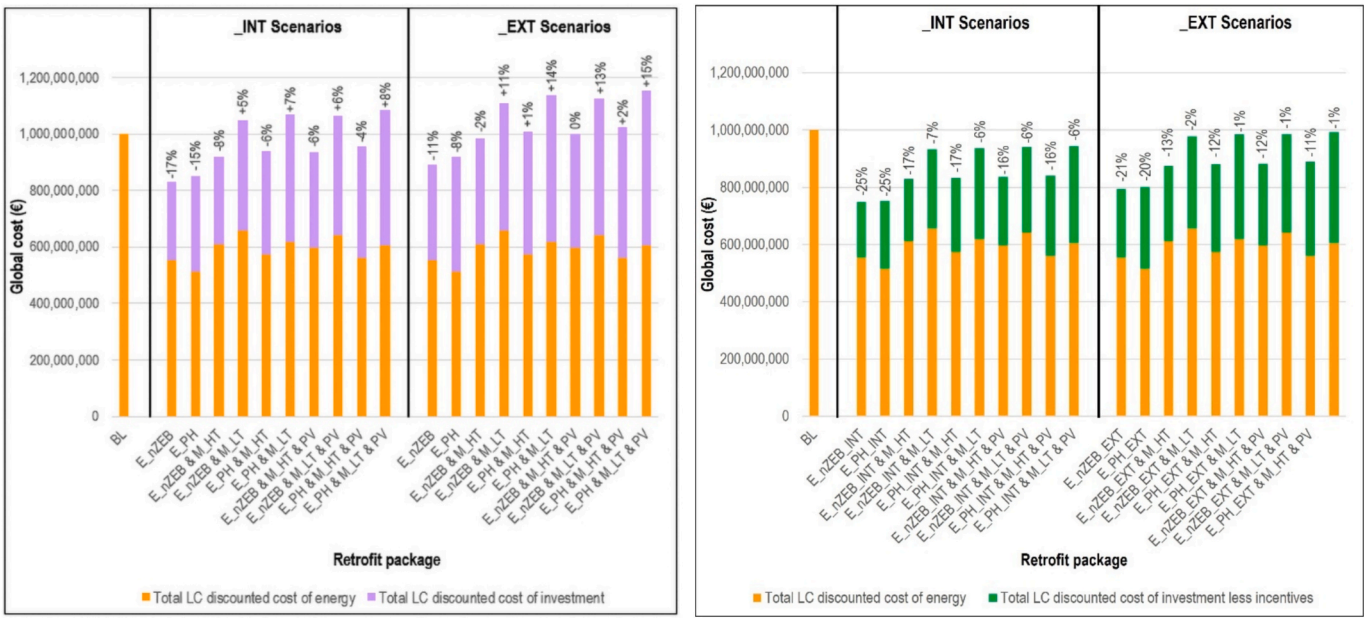


Fig. 10. Life cycle energy plus investment cost for all retrofit packages evaluated with no incentives (left) and the homeowner perspective with investment costs net of incentives (right). BL = baseline.
Source: authors' elaboration.

future perspectives for each.

6.1. *Energy simulation*

A limitation of the energy simulation employed, inter-building effects were not fully investigated. The URBANopt/EnergyPlus workflow evaluates shading by nearby buildings[68], within a 50-meter radius in this work. However, longwave radiation exchanges between buildings were not simulated. In a recent study at district scale, neglecting longwave radiation exchange led to annual energy variations of + 1.39% for cooling and −0.45% for heating[69]. A study at building scale found that simulations underpredict annual cooling demand up to 17% and overpredict heating demand up to 6%[70].

Another limitation, we did not investigate model uncertainties, such as weather, HVAC systems, and occupant patterns. Instead, the deterministic model generalizes these factors, which is typical for archetype-based simulations. A review of 61 UBEM articles found that nearly all works used standard TMY weather files, that simplified approaches to HVAC modeling with constant COPs are common, and that most works use fixed occupant schedules[71], mirroring this work's approach. There are challenges to incorporate stochastic models into UBEM, including high computational demands, algorithm complexity, large datasets, and significant processing power[72]. Changes in occupants' behavior could lead to energy savings of 6%-25% in residential buildings[73].

A final limitation, energy results could not be validated with consumption data, as utility companies cannot make these available due to European privacy regulations. Thus, validation could not be performed on a per-building basis, and instead was completed on an aggregated, per-archetype basis using two data sources.

The first uses TABULA energy performance data, including primary energy values for heating, DHW, and combined. TABULA excludes cooling, lighting, and equipment energy. Fig. 13 depicts the results against TABULA values for four AB and four MF archetypes, representing 78% and 9% of district GFA. For AB archetypes, mean differences from TABULA combined energy use are −12% (R3AB), −27% (R4AB), −14% (R5AB), and 8% (R6AB). MF archetypes show smaller variances, from −10% (R3MF, R4MF) to 13% and 14% (R5MF, R6MF). For all archetypes, weighted by district GFA, the simulations vary from TABULA by − 5% for heating, −35% for DHW, and − 11% combined.

Secondly, Fig. 13 compares results against energy performance values in URBEM, a recently completed project creating a national

Table 6
Results of LCC with deployment scenarios with constant EF. CDCF = cumulative discounted cash flow; RW = Renovation Wave scenario; 100CNC = 100 Climate-Neutral Cities scenario.

Retrofit package	RW – 2% per year					100CNC – 20% per year				
	Maximum CO_2 emissions reduction from baseline	_INT CDCF (million €)	CDCF per % CO_2 reduced (million €)	_EXT CDCF (million €)	CDCF per % CO_2 reduced (million €)	Maximum CO_2 emissions reduction from baseline	_INT CDCF (million €)	CDCF per % CO_2 reduced (million €)	_EXT CDCF (million €)	CDCF per % CO_2 reduced (million €)
E_nZEB	36%	668.5	18.4	699.3	19.2	51%	546.5	10.6	607.7	11.8
E_PH	40%	685.5	17.3	719.5	18.2	56%	568.8	10.1	635.0	11.3
E_nZEB & M_HT	49%	701.2	14.2	732.9	14.9	70%	652.3	9.3	713.5	10.2
E_PH & M_HT	50%	718.7	14.2	752.7	14.9	72%	672.1	9.3	738.3	10.3
E_nZEB & M_LT	48%	781.8	16.3	813.5	17.0	68%	864.3	12.7	925.5	13.6
E_PH & M_LT	49%	799.4	16.3	833.4	17.0	70%	884.0	12.7	950.2	13.6
E_nZEB & M_HT & PV	53%	716.2	13.5	747.8	14.1	76%	677.5	8.9	738.7	9.7
E_PH & M_HT & PV	54%	733.6	13.5	767.6	14.2	78%	697.4	9.0	763.6	9.8
E_nZEB & M_LT & PV	52%	796.7	15.4	828.4	16.0	74%	889.5	12.1	950.7	12.9
E_PH & M_LT & PV	53%	814.4	15.4	848.4	16.0	76%	909.2	12.0	975.4	12.9

Table 7
Results of LCC with deployment scenarios with variable EF. CDCF = cumulative discounted cash flow; RW = Renovation Wave scenario; 100CNC = 100 Climate-Neutral Cities scenario.

Retrofit package	RW – 2% per year				100CNC – 20% per year			
	Maximum CO_2 emissions reduction from baseline	Additional CO_2 reduction compared to constant EF scenario	_INT CDCF per % CO_2 reduced (million €)	_EXT CDCF per % CO_2 reduced (million €)	Maximum CO_2 emissions reduction from baseline	Additional CO_2 reduction compared to constant EF scenario	_INT CDCF per % CO_2 reduced (million €)	_EXT CDCF per % CO_2 reduced (million €)
E_nZEB	41%	5%	16.3	17.1	58%	6%	9.4	10.5
E_PH	45%	5%	15.3	16.0	64%	7%	8.9	10.0
E_nZEB & M_HT	69%	19%	10.2	10.7	100%	30%	6.5	7.1
E_PH & M_HT	69%	18%	10.5	11.0	100%	28%	6.7	7.4
E_nZEB & M_LT	69%	21%	11.4	11.8	100%	32%	8.6	9.3
E_PH & M_LT	69%	20%	11.6	12.1	100%	30%	8.8	9.5
E_nZEB & M_HT & PV	69%	16%	10.4	10.9	100%	24%	6.8	7.4
E_PH & M_HT & PV	69%	14%	10.7	11.2	100%	22%	7.0	7.6
E_nZEB & M_LT & PV	69%	17%	11.6	12.1	100%	26%	8.9	9.5
E_PH & M_LT & PV	69%	16%	11.9	12.4	100%	24%	9.1	9.8

database of building archetypes [75]. In Piedmont climate zone 'E', the URBEM "scorecards" list energy performance certificates as 100% of the source data, meaning these are based on energy simulations under standard assumptions for each subject building, as in this study, and not on actual consumption data. The figure reconciles differences in building types (URBEM has only one apartment type) and aligns time periods as closely as possible to the results despite mismatches between time steps. For combined energy use, the median for AB buildings was within the interquartile range of the URBEM values for R3AB and R6AB, and around the URBEM Q3 value for the middle two eras. MF building medians were generally above the URBEM interquartile range, except for R6MF which aligns across both studies. Energy performance is significantly higher in this study than in URBEM for building years 1931 to 1970, with median differences from URBEM of 47%, 22%, 42%, and − 22% for R3AB–R6AB, and 54%, 65%, 50%, and − 5% for R3MF–R6MF.

Overall, the results aligned closely with TABULA averages for

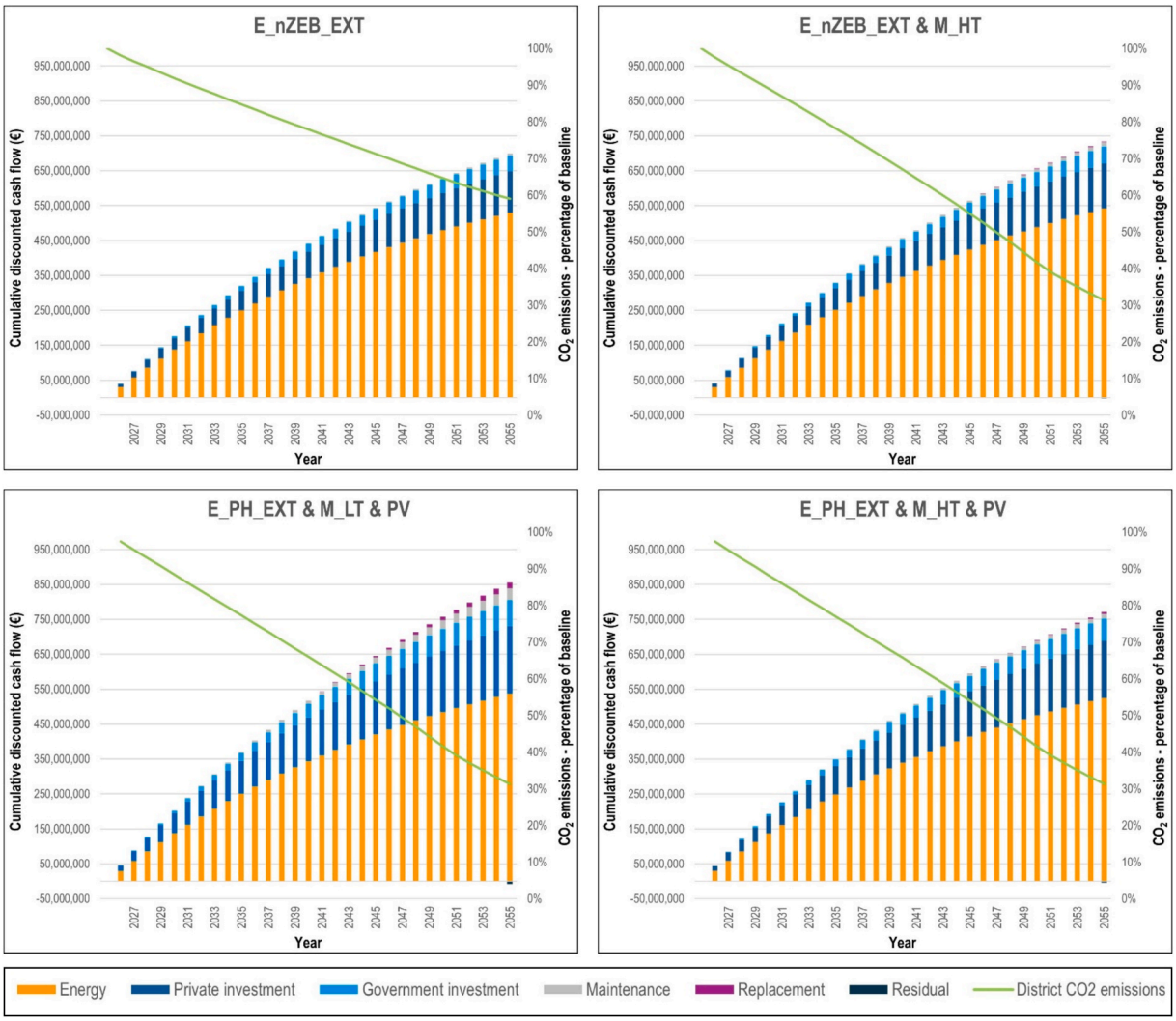


Fig. 11. CDCF through 2054 and CO_2 as a percentage of baseline emissions, in the Renovation Wave scenario (2% retrofit rate) with variable EF. Costs are broken down by source per the legend at bottom.
Source: authors' elaboration.

heating and combined energy use, and are significantly higher than URBEM values. If the present results overestimate baseline consumption, then actual energy savings may be lower, since large energy savings are easily achieved from a starting point of high consumption, inverse to the law of diminishing returns.

To address possible simulation error from lack of complete validation and from neglecting longwave radiation exchange between buildings, the next subsection presents a sensitivity analysis to show the financial impact of greater or lesser energy savings than simulated.

For future research, we note to policymakers that anonymized consumption data should be made available to enable complete validation of simulation results and to facilitate modeling and validation of occupancy-related parameters, HVAC systems, and other model parameters.

6.2. *Sensitivity analysis*

We conducted a sensitivity analysis using the OAT (One-At-a-Time) approach, where one input parameter is varied at a time, while all other parameters are held constant, to assess how changes in that single variable affect the model's output. The approach identifies the individual influence of each parameter, helping to evaluate the robustness of the model to uncertainties in its assumptions.

First is a sensitivity analysis for energy savings and global cost. Fig. 14 (a) and (b) vary total energy use for the district by −20% to + 20%, where 0% means no variation from simulation results and costs are identical to those in Fig. 10. The baseline energy values are also varied by the amount shown at each data point. The figure depicts the EXT scenarios only, though trends for INT scenarios are identical. In all scenarios, a decreasing trend is evident, showing that overestimated energy savings decrease retrofit profitability. For the analysis including incentives (i.e. the homeowner's perspective), if actual energy use is 20% less than simulated, six retrofit packages (envelope-only and those adding high-temperature HPs) are still profitable, representing savings of 3% to 15% global cost compared to baseline. From a public policy standpoint, government incentives for these packages would be considered worthwhile, as they achieve decarbonization goals and provide cost savings to homeowners. The packages including low-temperature HPs become more expensive than baseline by 6% to 9% on a global cost basis. Without incentives, if actual energy use is 20% less than simulated, nearly all packages are more expensive than the baseline scenario.

Similarly, the second sensitivity analysis varies investment cost by −20% to + 20%, where 0% are the same as costs reported in Table 5, and incentives are modulated by the same percentage. With incentives, the same six packages (envelope-only or with added high-temperature HPs)

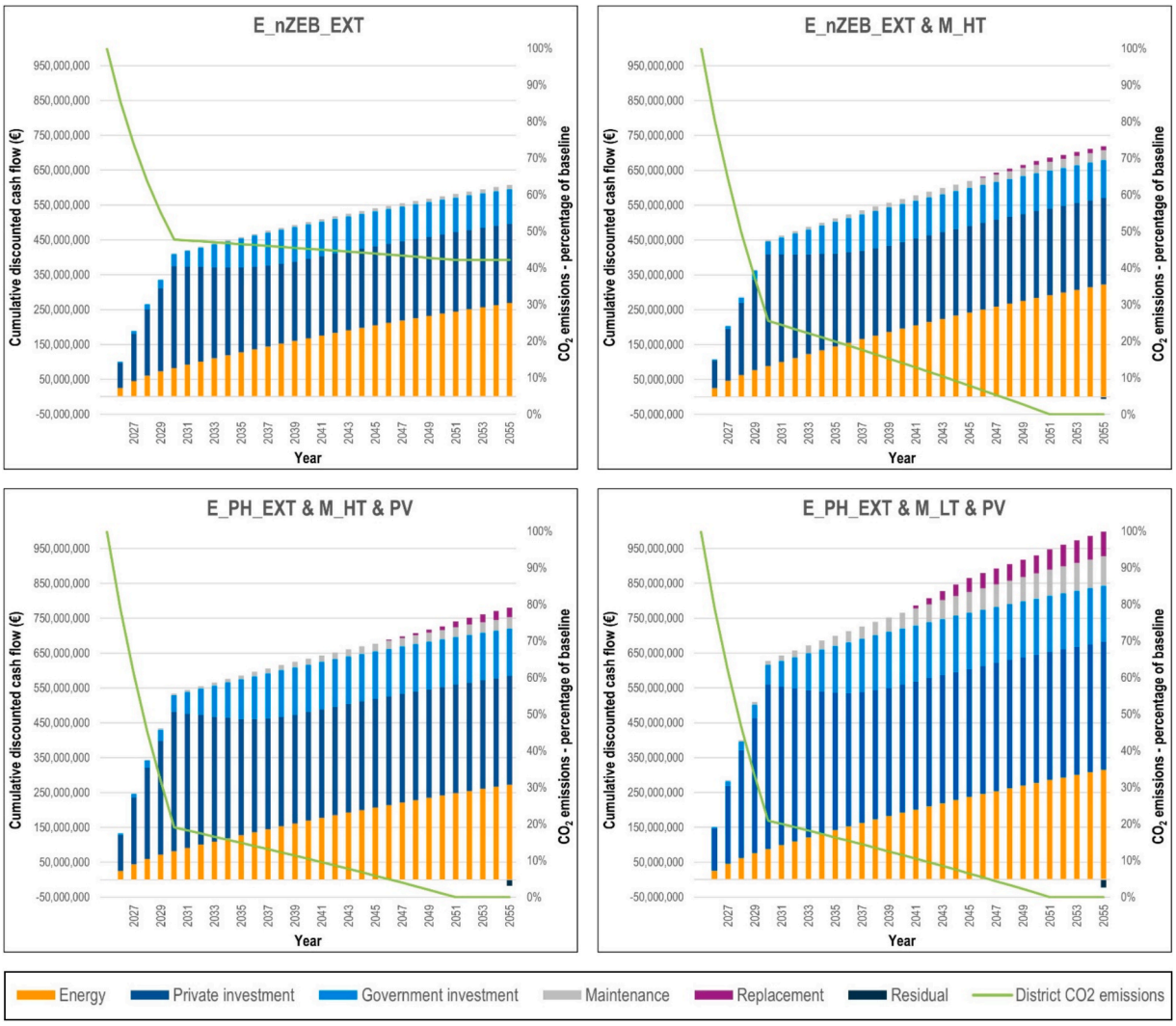


Fig. 12. CDCF through 2054 and CO_2 as a percentage of baseline emissions, in the 100 Climate-Neutral Cities scenario (20% retrofit rate) with variable EF. Costs are broken down by source per the legend at bottom.
Source: authors' elaboration.

are profitable even with an investment cost increase of 20%.

We also conduct a sensitivity analysis for GC in response to discount and energy inflation rate variations. Fig. 14 (c) and (d) show that GC increases steadily with discount rates for all packages. At a discount of 0% and no incentives, all packages are profitable. At discount rates of 2%-4%, all except envelope-only packages cease to be profitable. With incentives, the more comprehensive packages remain profitable until discount rates of 7%-9% are reached. For sensitivity of energy prices in Figure (e) and (f), the trends occur in the opposite direction with similar magnitudes of percentage difference in GC compared to baseline, where high energy inflation leads to high future energy prices, increasing profitability of energy-saving retrofits.

Overall, the sensitivity analysis confirms that our approach yields consistent rankings, even when key assumptions—such as energy consumption patterns, investment costs, discount rates, and future energy-price trajectories—are varied within reasonable uncertainty ranges.

6.3. Automatic envelope detection

The urban sensing and AI techniques used to determine investment costs have the advantage of speed in calculations, amounting to approximately 16 h to extract and prepare images for window detection, 2 h for the complete roof workflow, and 10 min to separate exterior from party walls, with acceptable levels of accuracy. Previous research showed that 94% of façade detections were within ± 5% of the ground truth WWR[37]. The present work did not quantify accuracy of the existing Dragonfly tool to isolate exterior walls from interior walls, though the sample in Fig. 6 shows that most, but not all, walls are detected correctly. In any case, we believe this to be an improvement on the status quo, as distinguishing exterior and adjoining walls is otherwise challenging with standard GIS-to-UBEM workflows.

With −10.4% error, the roof workflow is acceptable for investment cost calculation purposes. Without the workflow, roof surfaces could be constructed directly from LiDAR points with standard GIS tools, but such roof surfaces can be distorted by chimneys or other rooftop elements, leading to excessive surface area. Instead, our novel workflow models simplified roof surfaces with an effective result. The workflow did not account for roof overhangs, perhaps explaining why true roof areas are greater than detected. This explanation is supported by higher error rates observed in detached buildings, which have overhangs on all sides, and buildings with four vertices, where roof overhangs lead to greater error on the smaller roof surfaces. As noted, the existing roof classifier was limited to three shapes (flat, gable, and hip roof), which does not capture the roofs with one hip and one gable end present in the district nor other complex roof shapes, and this could decrease the accuracy of the geometry generation.

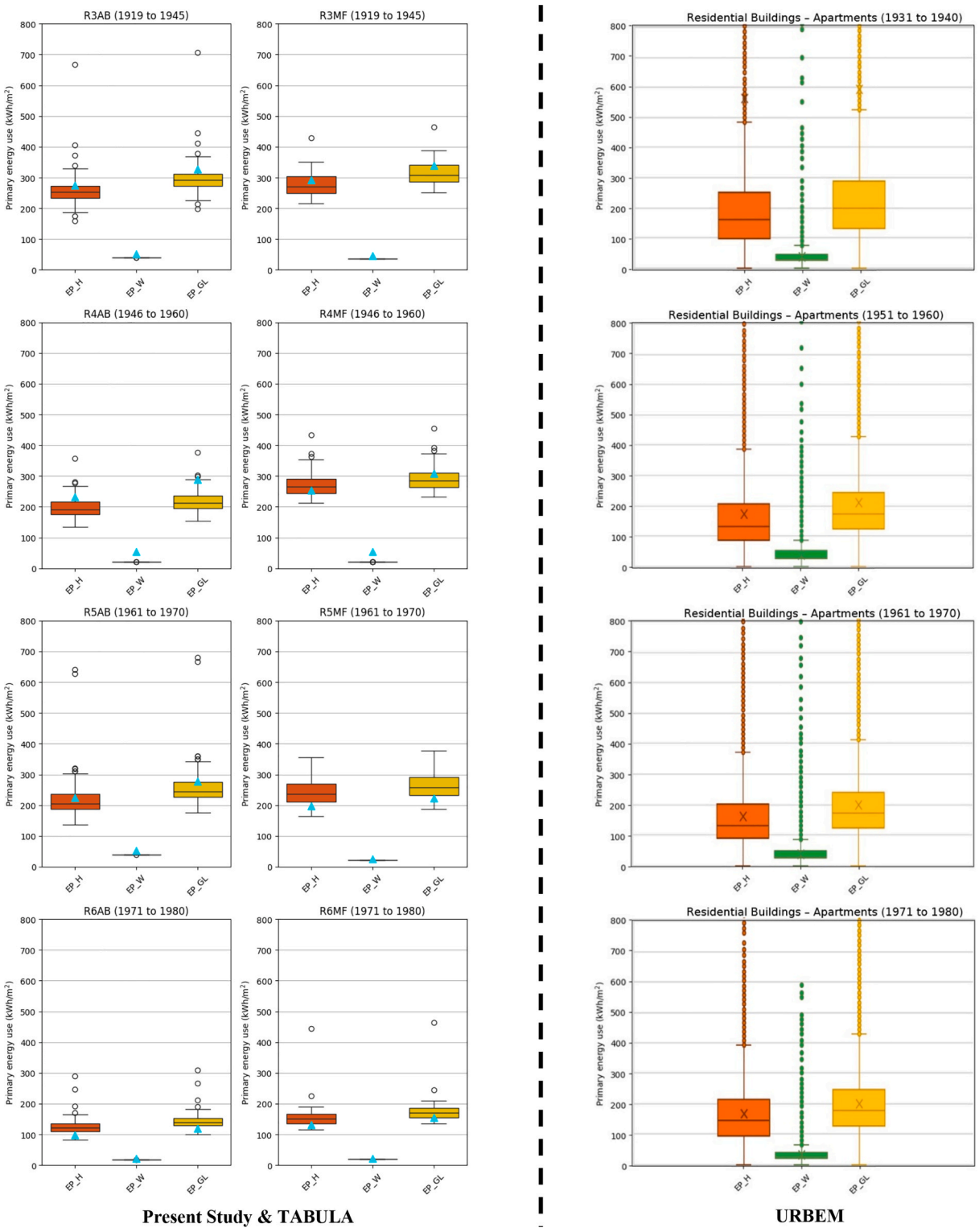


Fig. 13. Validation of energy performance (EP) for heating (_H), DHW (_W), and combined (_GL). Left: EP distribution for predominant archetypes against averages in TABULA (cyan triangles); source: authors' elaboration. Right: EP distribution from URBEM "scorecards" for corresponding building types; source: [74]. (For interpretation of the references to colour in this figure legend, the reader is referred to the web version of this article.)

To address limitations of the roof workflow, future research could improve the Grasshopper-based roof script to incorporate overhangs, accounting for whether buildings are detached/attached, to potentially reduce roof area error. Future research could also incorporate deep learning tools, which have been used to classify roof types[76] or define roof structure lines[77]. With district roof retrofit costs of €60 million greater when completed from the exterior, it is valuable to have accurate roof quantities in urban-scale LCC. While this study quantified costs in EXT and INT scenarios—the high and low ends of the range—the reality lies somewhere in between. A deep-learning-based classifier might detect whether a roof has skylights or dormers, strong indications of an inhabited attic, which necessitate insulation from the exterior. Such a

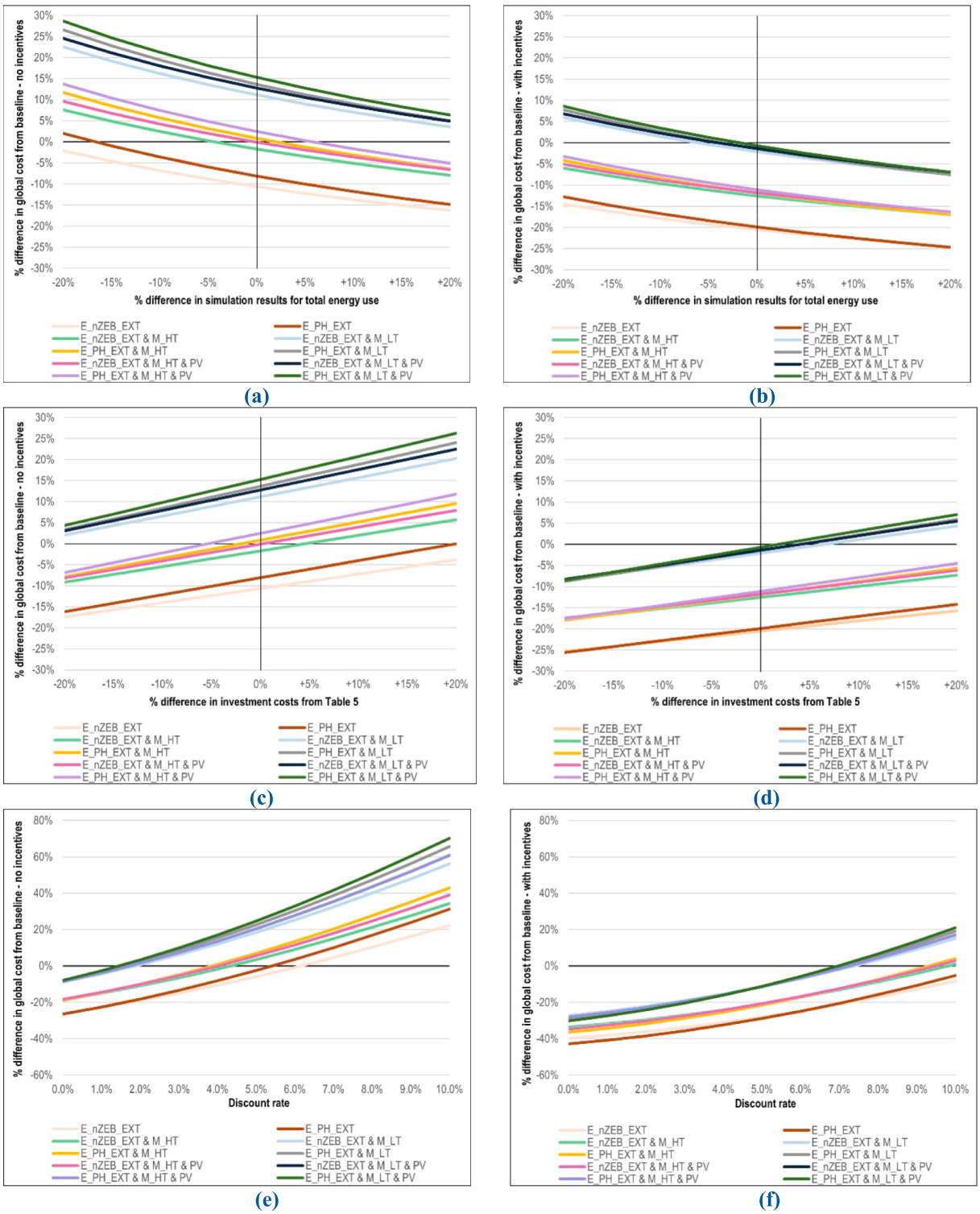
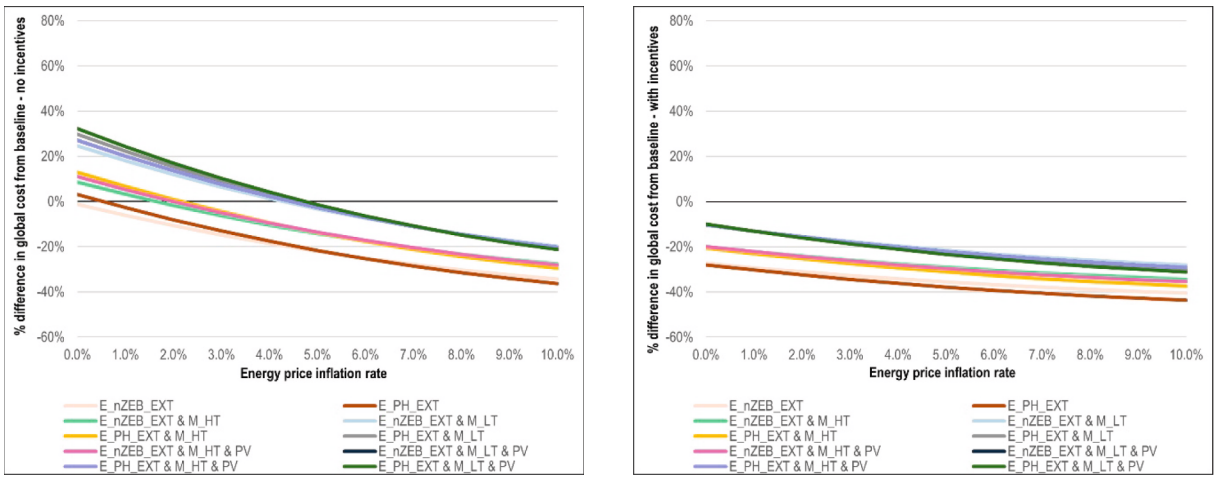


Fig. 14. Sensitivity analysis for GC and variations in energy simulation results, discount rate, or energy inflation rate. In (a) and (b), total annual energy use ranges from −20% to + 20%, and in (c) and (d) the investment costs vary from −20% to + 20%; in both cases, 0% is the equal to the results presented in Section 5. In (e) and (f), discount rates vary while holding the energy inflation rate constant at 2%. In (g) and (h), energy inflation rates vary while the discount rate is held constant at 4%. Source: authors' elaboration

classifier might also improve upon the one used in this work, which was less effective on hip roofs with more than four vertices and on roofs with mixed hips and gables.

A final advantage of the presented envelope workflows is scalability to other districts or cities, aligning with the Renovation Wave and EPBD policies, which emphasize accelerating retrofits across multiple building types in districts. The roof workflow could likely be applied to other contexts, since it was tested on diverse building geometries, including dense blocks with attached rectangles at mid-block and various L-shapes with non-right angles at corner positions, as well as detached and semi-



(g) (h)

Fig. 14. (*continued*).

detached geometries in less dense areas. Similarly, our previous research noted that the window workflow could be applied beyond the context of Turin, but limited to masonry buildings with punched windows, unless the model is further trained and tested on other architectural forms[37]. The Dragonfly tool to separate adjoining party walls is intended for any context. Thus, the envelope workflows could be integrated into urban-scale energy and cost models beyond the context of the case study presented.

6.4. Cost, energy, and emissions

Results specific to the case study show that combining envelope and mechanical retrofits consistently led to greater CO_2 reductions, with 68% or more CO_2 savings under the current electricity supply, and zero emissions under the variable EF scenario. Packages combining envelope retrofits with high-temperature HPs also have the lowest CDCF per CO_2 reduction. All costs and energy savings reported must be limited to the case study in Turin, Italy.

The case study results also present complex outcomes considering diverse deployment scenarios. While envelope-only packages were the most profitable in the GC analysis, these have a greater CDCF to reduce each percentage of baseline CO_2 emissions. The lower global costs can be partly attributed to the low cost of gas, less than one-third of the cost of electricity per kWh in Italy. A drawback of envelope-only retrofits was evident when applying variable EF scenarios, as buildings retrofitted with envelope-only packages continue to emit CO_2 from gas combustion for heating, whereas CO_2 from electrified heating systems approaches zero as the electrical grid is decarbonized. The latter also applies to contexts beyond Italy, with most G20 countries aiming for decarbonization by 2050.

Furthermore, the CDCF analysis showed that, for six of the 10 retrofit packages, accelerating retrofits under the 100CNC scenario led to lower overall CDCF compared to the RW scenario. This is even though 100% of the case study is retrofitted in the former scenario (1.4 million m^2 of GFA) and only 61% (around 855,000 m^2) in the latter scenario. While one can question the likelihood of such accelerated retrofits within five years for a large district, the implication is that faster and earlier retrofitting can lead to greater cost savings over time. This highlights the value of LCC in scenario analysis to reduce overall costs and maximize CO_2 reductions while assessing retrofit deployment.

Other context-specific results may have implications beyond Italy. The retrofit investment costs calculated at €13,723 to €27,272 per dwelling are significantly higher than the €11,340 per dwelling that would be budgeted for the district under the EU mission 100 Climate-Neutral Cities.[3] While this cost result is limited to the case study, the method of calculating urban-scale life cycle costs and energy use is valid for other EU contexts, and could have important implications for the 100 cities (in 27 countries) participating in the EU mission.

Furthermore, the sensitivity analysis of energy prices in Section 6.2 has implications beyond Italy, with marked increases in retrofit profitability as energy costs rise. Across the EU, energy prices include carbon pricing under the EU Emissions Trading System, currently around 70 €/tonne of CO_2. We excluded CO_2 cost from the GC analysis to avoid double-counting within energy cost. Notably, some forecasters have predicted sharp increases in CO_2 prices, potentially rising to 500 €/tonne by 2044 [78], representing an annualized inflation rate of 10%. Such CO_2 prices would exert heavy upward pressure on energy prices, making energy-saving retrofits more profitable across the EU.

7. Conclusion

This work combined life cycle costing with energy modeling for district-scale building retrofits. To our knowledge, it is the first study to conduct urban-scale LCC at LOD3, enriched with envelope data extracted using advanced urban sensing and AI techniques.

Windows were detected using deep learning and street view images. Roof areas were quantified in a novel workflow using a classifier in ArcGIS based on LiDAR data and a custom script in Rhino/Grasshopper to model roof geometries. Exterior walls were separated from party walls in adjoining buildings to determine wall insulation quantities, using a novel application of an existing Dragonfly tool. These technologies allow for rapid and accurate capture of envelope quantities, to which we applied unit costs to calculate investment costs in the LCC.

Energy consumption in pre- and post-retrofit conditions was calculated using UBEM, conducting dynamic simulations on a floor-by-floor basis for each building in the case district. The UBEM can be considered LOD1+, with flat roof geometries and detected window areas.

A total of 80 scenarios were modeled, including 10 retrofit packages, two scenarios for roof renovation, and four deployment scenarios. The latter includes retrofit deployment at rates of 2% and 20% to meet the EU Renovation Wave policy and the EU mission 100 Climate-Neutral Cities, respectively, using emission factors for the current electricity

[3] The mission budget is €10,000 per citizen for all sectors, of which €5,400 is budgeted for buildings [2]. Assuming EN-16798–1 [80] occupancy rates of 28.3 m2 per person, the average 60 m^2 dwelling in the case study has approximately 2.1 inhabitants, translating to an EU retrofit budget of €11,340 per dwelling.

supply and a steadily decarbonizing supply by 2050.

Results specific to the case study show complex outcomes considering diverse retrofit deployment scenarios, though in all scenarios, packages including envelope retrofits and high-temperature heat pumps led to the greatest CO_2 emission savings, and the lowest cumulative discounted cash flow per quantity of CO_2 saved. While envelope-only retrofit packages had the lowest global cost, they are the most expensive when it comes to cost to reduce each percentage of CO_2 emissions from baseline. The findings highlight the value of faster and earlier retrofits at urban scale, as accelerated retrofit deployment under 100CNC (20% of the building stock per year) resulted in lower cumulative discounted cash flow by 1–18%, depending on the retrofit pacakage, compared to the RW scenario (2% per year). This is despite the fact that the 100CNC scenario envisages nearly 550,000 m^2 more retrofitted floor area than the RW scenario - a 64% increase in GFA).

The present findings have implications for the City of Turin and beyond. For Turin, an extensive set of retrofit packages and deployment scenarios has been modeled for cost, energy, and emissions, resulting in significantly higher costs than budgeted in the EU mission 100 Climate Neutral Cities. The budget overrun highlights the need to strengthen incentives such as Ecobonus in Italy and similar programs elsewhere, and to develop long-term financing tools for deep energy retrofitting. Other cities, especially those in the EU mission facing similar budget constraints, could adopt the methodologies of this research, including urban-scale LCC and energy analysis to model context-appropriate retrofits and local costs. Other cities could also test retrofit deployment rates, and while a 20% rate might be overly ambitious or unachievable, it is worth testing the finding that faster and earlier retrofits can lead to greater savings in other contexts.

Supporting research beyond the case study, the automatic envelope quantity extraction workflows of this work are made publicly available. The workflows can be applied in diverse contexts outside of the case study, since the window workflow was tested in diverse geographies (limited to masonry buildings with punched windows), the roof workflow was tested on multiple geometries including simple rectangular and complex shapes plus attached and detached buildings, and the workflow separating exterior and party walls derives from a tool within the Dragonfly plug-in intended for any geometry. As demonstrated in this work, the automatic envelope workflows add detail and accuracy to urban-scale energy and LCC models.

At the EU and global levels, this study highlights the value of incorporating advanced urban sensing and AI techniques to plan district-scale retrofits. Such techniques enable governments in diverse regions to balance costs against energy improvement needs, especially in critical areas in terms of energy consumption and emissions, facilitating evidence-based decisions to achieve climate goals.

With decarbonization deadlines fast approaching, policymakers must decide where priorities lie and where to use incentives and other policy tools. Combining energy, emissions, and cost analysis for district-scale retrofit scenarios, as conducted in this study, can support decision-making for policymakers guiding a rapid transition to climate neutrality.

CRediT authorship contribution statement

Anthony Robert Suppa: Writing – review & editing, Writing – original draft, Visualization, Validation, Software, Resources, Project administration, Methodology, Investigation, Formal analysis, Data curation, Conceptualization. **Marta Carla Bottero:** Writing – review & editing, Supervision. **Vincenzo Corrado:** Writing – review & editing, Supervision. **Federico Dell'Anna:** Writing – review & editing, Methodology, Investigation.

Declaration of competing interest

The authors declare that they have no known competing financial interests or personal relationships that could have appeared to influence the work reported in this paper.

Acknowledgment

This research did not receive any specific grant from funding agencies in the public, commercial, or not-for-profit sectors. The authors thank Jordan Goldman of ZeroEnergy Design for consultation on retrofit designs and energy simulations, as well as the anonymous reviewers for their constructive comments and feedback.

Data use statement

The street view dataset used is confidential. Google Street View and Google Earth data have been used further to European Union Directive 2019/790 on copyright and related rights in the Digital Single Market, and its national implementation in Italian law, the legislative decree of 8 November 2021, n. 177. Due to Google copyright on GSV images, all street view images printed in this work are facsimiles of the GSV images, using photos taken by the authors.

Appendix

.

Table A1
. Retrofit life span and maintenance cost used in the LCC. Sources: (1) [18], using upper range values where applicable; (2) [30].

Component	Life span (years)	Annual maintenance cost, percentage of investment cost (%)
Windows, wood	30 (1)	1 (1)
Windows, PVC	30 (1)	0.5 (1)
Insulation to roof/floor/walls	40 (2)	0 (2)
Control valves, automatic	15 (1)	6 (1)
Fan coil units	15 (1)	4 (1)
Electric wiring to fan coils	50 (1)	1 (1)
Heat pumps	20 (1)	4 (1)
Piping systems	30 (1)	1 (1)
Pumps – circulation	20 (1)	2 (1)
Heated & chilled buffer tanks	20 (1)	1 (1)
Solar panels	25 (1)	0.5 (1)

Table A2
. Additional costs associated with retrofit work. MC = maintenance costs, calculated as a percentage of investment cost; LS = life span. Sources: (1) [60], (2) [51]; (3) [20]; (4) [79].

Item	Description	Unit costs	Quantity / Sizing	MC (%)	LS (years)
Waste disposal & transport	Transport of waste from site and disposal.	Waste (4): Wood 140.68 €/tonne Inert 10 €/tonne Non-hazardous 20 €/tonne Transport: 12 €/tonne Radiator removal: 40 € each (1)	Estimate kg of waste per m^2 of wall, roof, and window retrofits plus a general waste estimate based on GFA. For low-temp HP scenario, include cost to remove radiators equal to number of added fan coils.	n/a	n/a
Scaffolding	Rental, installation, and removal of scaffold frames and platforms to complete exterior insulation works.	Frames: 19.22 € per m^2 (first month) and 3.24 € per m^2 (additional months) (1) Platforms: 3.04 € per m^2 (1)	Frame surface equal to wall insulation area plus 1-meter-wide platform at each floor; duration in months equal to number of floors plus 1.	n/a	n/a
Condensate drainage	*For low-temp HP scenario only:* cost to provide condensate drainage for fan coils, including PVC piping, fittings, pipe supports, drilling & patching.	SF & TH (1): 461.77 € per floor+ 28.93 € per (height x floors) AB & MF (1): 610.52 € per unit + 25.77 € per façade length+ 28.93 € per (no. units / no. floors x bldg height)	Assume separate riser piping for vertically stacked units, installed at building exterior and integrated with façade retrofits. Cumulative sum based on building height, no. floors, no. units, façade length, and multiplied by unit costs from (1).	0.5% (3)	30 (3)
Fan coil wiring	*For low-temp HP scenario only:* cost for electrical conduit and wiring for FCs.	59.65 € per FC (1)	Assume 5 m per fan coil	0.5% (3)	50 (3)
HP mode switching costs	*For low-temp HP scenario only:* cost for motorized valves, pumps, and chilled buffer tanks to switch between DHW and space cooling modes.	Valves & pumps: SF & TH: 567 € per bldg (1) AB & SF: 797 € per bldg (1) Tanks:461.43 € (200 L) to 2,270.72 € (2,000 L) (2)	Assume one motorized valve per building, 100 W pump, with 5 m conduit and wire each, chilled buffer tank based on 20 L per kW cooling.	Valves: 4% (3) Pumps: 2% (3) Tanks: 1% (3)	Valves: 15 (3) Pumps: 20 (3) Tanks: 20 (3)
Heated and chilled storage tank	*For archetypes with no existing DHW storage tank:* new heated storage tanks. *For all other archetypes:* insulate existing storage tanks. *All low-temp scenarios:* new chilled storage tank.	New tanks:461.43 € (200 L) to 2,270.72 € (2,000 L) (2) Insulate existing tanks: 90.44 € per m^2 tank surface (1)	Size based on the greater of half day's DHW supply for each building (DHW flow rate from EN 16798–1:2019) or 20 L per kW heating. 20 L per kW cooling.	1% (3)	20 (3)
Convert DHW system to centralized	*For MF & AB archetypes with existing autonomous DHW systems only:* cost for centralized DHW piping. Includes copper piping, fittings, pipe supports, pipe insulation, drilling & patching, expansion tanks, circulation pumps, installation allowance.	Pump: 1,160.23 (1) Piping system (1): 1,639.03 € per bldg + 452.45 € per unit + 89.78 € per floor + 95.59 € per façade length+ 59.26 € per (no. units / no. floors x bldg height)	Assume separate riser piping for vertically stacked units, installed at building exterior and integrated with façade retrofits. Risers connected in closed loop at top & bottom. Cumulative sum based on building height, no. floors, no. units, façade length, and multiplied by unit costs from (1).	Piping system: 0.5% (3) Pumps: 2% (3)	Piping system: 30 (3) Pumps: 20 (3)
Convert heating system to centralized	*For MF & AB archetypes with existing autonomous heating systems only:* cost for centralized supply and return heating piping. Includes copper piping, fittings, pipe supports, pipe insulation, drilling & patching, circulation pumps, installation allowance.	Pump: 1,160.23 (1) Piping system (1): 1,295.66 € per bldg + 616.93 € per unit + 161.25 € per floor + 189.85 € per façade length+ 117.17 € per (no. units / no. floors x bldg height)	Assume separate twinned riser piping for vertically stacked units, installed at building exterior and integrated with façade retrofits. Risers connected in closed loop at top & bottom. Cumulative sum based on building height, no. floors, no. units, façade length, and multiplied by unit costs from (1).	Piping system: 0.5% (3) Pumps: 2% (3)	Piping system: 30 (3) Pumps: 20 (3)

Data availability

The authors do not have permission to share data.

References

[1] McKinsey & Company. (2023). The net-zero transition: what it would cost, what it could bring. [Online]. https://www.mckinsey.com/capabilities/sustainability/our-insights/the-net-zero-transition-what-it-would-cost-what-it-could-bring#/download/%2F~%2Fmedia%2Fmckinsey%2Fbusiness%20functions%2Fsustainability%2Four%20insights%2Fthe%20net%20zero%20transition%20what%20it%20would%20cost%20what%20it%20could%20bring%2Fthe-net-zero-transition-what-it-would-cost-and-what-it-could-bring-final.pdf.

[2] European Commission (EC). (2020a). Proposed Mission: 100 Climate-neutral Cities by 2030 – by and for the Citizens. Report of the Mission Board for climate-neutral and smart cities. Luxembourg: Publications Office of the European Union.

[3] European Commission (EC). (2020b). A Renovation Wave for Europe - greening our buildings, creating jobs, improving lives. COM(2020) 662 final. Brussels: European Commission.

[4] European Union (EU). (2024). Directive 2024/1275 of the European Parliament and of the Council of 24 April 2024 on the energy performance of buildings (recast). Brussels: Official Journal of the European Union.

[5] C.F. Reinhart, C.C. Davila, Urban building energy modeling–a review of a nascent field, Building and Environment 97 (2016) 196–202, https://doi.org/10.1016/j.buildenv.2015.12.001.

[6] T. Hong, Y. Chen, X. Luo, N. Luo, S.H. Lee, Ten questions on urban building energy modeling, Building and Environment 168 (2020) 106508, https://doi.org/10.1016/j.buildenv.2019.106508.

[7] A.R. Suppa, I. Ballarini, Supporting climate-neutral cities with urban energy modeling: a review of building retrofit scenarios, focused on decision-making, energy and environmental performance, and cost, Sustainable Cities and Society 98 (2023) 104832, https://doi.org/10.1016/j.scs.2023.104832.

[8] C. Wang, M. Ferrando, F. Causone, X. Jin, X. Zhou, X. Shi, Data acquisition for urban building energy modeling: a review, Building and Environment 217 (2022) 109056, https://doi.org/10.1016/j.buildenv.2022.109056.

[9] M. Ferrando, F. Causone, T. Hong, Y. Chen, Urban building energy modeling (UBEM) tools: A state-of-the-art review of bottom-up physics-based approaches, Sustainable Cities and Society 62 (2020) 102408, https://doi.org/10.1016/j.scs.2020.102408.

[10] F. Ascione, N. Bianco, G.M. Mauro, D.F. Napolitano, Knowledge and energy retrofitting of neighborhoods and districts. a comprehensive approach coupling geographical information systems, building simulations and optimization engines, Energ. Conver. Manage. 230 (2021) 113786, https://doi.org/10.1016/j.enconman.2020.113786.

[11] C. Delmastro, G. Mutani, S.P. Corgnati, A supporting method for selecting cost-optimal energy retrofit policies for residential buildings at the urban scale, Energy Policy 99 (2016) 42–56, https://doi.org/10.1016/j.enpol.2016.09.051.

[12] L. Liu, P. Rohdin, B. Moshfegh, Investigating cost-optimal refurbishment strategies for the medieval district of Visby in Sweden, Energy and Buildings 158 (2018) 750–760, https://doi.org/10.1016/j.enbuild.2017.10.002.

[13] U. Ali, M.H. Shamsi, C. Hoare, E. Mangina, J. O'Donnell, Review of urban building energy modeling (UBEM) approaches, methods and tools using qualitative and quantitative analysis, Energ. Buildings 246 (2021) 111073, https://doi.org/10.1016/j.enbuild.2021.111073.

[14] Y. Chen, T. Hong, X. Luo, B. Hooper, Development of city buildings dataset for urban building energy modeling, Energy and Buildings 183 (2019) 252–265, https://doi.org/10.1016/j.enbuild.2018.11.008.

[15] F. Johari, G. Peronato, P. Sadeghian, X. Zhao, J. Widén, Urban building energy modeling: State of the art and future prospects, Renewable and Sustainable Energy Reviews 128 (2020) 109902, https://doi.org/10.1016/j.rser.2020.109902.

[16] F. Biljecki, H. Ledoux, J. Stoter, An improved LOD specification for 3D building models, Comput. Environ. Urban Syst. 59 (2016) 25–37, https://doi.org/10.1016/j.compenvurbsys.2016.04.005.

[17] R. Nouvel, M. Zirak, V. Coors, U. Eicker, The influence of data quality on urban heating demand modeling using 3D city models, Computers, Environment and Urban, Systems 64 (2017) 68–80, https://doi.org/10.1016/j.compenvurbsys.2016.12.005.

[18] H. Harter, B. Willenborg, W. Lang, T.H. Kolbe, Climate-neutral municipal building stock-life cycle assessment of large residential building stocks based on semantic 3D city models, Energy and Buildings 292 (2023) 113141, https://doi.org/10.1016/j.enbuild.2023.113141.

[19] H. Harter, B. Willenborg, W. Lang, T.H. Kolbe, Life Cycle Assessment of building energy systems on neighbourhood level based on semantic 3D city models, Journal of Cleaner Production 407 (2023) 137164, https://doi.org/10.1016/j.jclepro.2023.137164.

[20] European Committee for Standardization (CEN) (2017). *Energy Performance of Buildings – Economic evaluation procedure for energy systems in buildings.* (EN 15459-1).

[21] European Union (EU). (2012a). Commission delegated regulation No. 244/2012 of 16 January 2012 supplementing Directive 2010/31/EU of the European Parliament and of the Council on the energy performance of buildings by establishing a comparative methodology framework for calculating cost-optimal levels of minimum energy performance requirements for buildings and building elements. Brussels: Official Journal of the European Union.

[22] European Union (EU). (2012b). Directive 2010/31/EU of the European Parliament and of the Council of 19 May 2010 on the energy performance of buildings (recast). Brussels: Official Journal of the European Union.

[23] A. Aslan, B. Yüksel, T. Akyol, Energy analysis of different types of buildings in Gonen geothermal district heating system, Appl. Therm. Eng. 31 (14–15) (2011) 2726–2734, https://doi.org/10.1016/j.applthermaleng.2011.04.044.

[24] R. Barbosa, M. Almeida, R. Briones-Llorente, R. Mateus, Environmental performance of a cost-effective energy renovation at the neighbourhood scale—The case for social housing in Braga, Portugal, Sustainability 14 (4) (2022) 1947, https://doi.org/10.3390/su14041947.

[25] C. Becchio, M.C. Bottero, S.P. Corgnati, F. Dell'Anna, Decision making for sustainable urban energy planning: an integrated evaluation framework of alternative solutions for a NZED (Net Zero-Energy District) in Turin, Land Use Policy 78 (2018) 803–817, https://doi.org/10.1016/j.landusepol.2018.06.048.

[26] S. Di Turi, P. Stefanizzi, Energy analysis and refurbishment proposals for public housing in the city of Bari, Italy, Energy Policy 79 (2015) 58–71, https://doi.org/10.1016/j.enpol.2015.01.016.

[27] J. Fernandez-Luzuriaga, L. del Portillo-Valdes, I. Flores-Abascal, Identification of cost-optimal levels for energy refurbishment of a residential building stock under different scenarios: Application at the urban scale, Energy and Buildings 240 (2021) 110880, https://doi.org/10.1016/j.enbuild.2021.110880.

[28] F. Haneef, G. Pernigotto, A. Gasparella, J.H. Kämpf, Application of urban scale energy modelling and multi-objective optimization techniques for building energy renovation at district scale, Sustainability 13 (20) (2021) 11554, https://doi.org/10.3390/su132011554.

[29] G. Luddeni, M. Krarti, G. Pernigotto, A. Gasparella, An analysis methodology for large-scale deep energy retrofits of existing building stocks: Case study of the Italian office building, Sustainable Cities and Society 41 (2018) 296–311, https://doi.org/10.1016/j.scs.2018.05.038.

[30] É. Mata, J. Wanemark, M. Österbring, F. Shadram, Ambition meets reality–Modeling renovations of the stock of apartments in Gothenburg by 2050, Energy and Buildings 223 (2020) 110098, https://doi.org/10.1016/j.enbuild.2020.110098.

[31] O. Pasichnyi, F. Levihn, H. Shahrokni, J. Wallin, O. Kordas, Data-driven strategic planning of building energy retrofitting: the case of Stockholm, Journal of Cleaner Production 233 (2019) 546–560, https://doi.org/10.1016/j.jclepro.2019.05.373.

[32] V. Corrado, I. Ballarini, S.P. Corgnati, N. Talà, *TABULA Project – Italy, Building Typology Brochure*, Department of Energy, Politecnico di Torino, Turin, 2011.

[33] J. Fernandez, L. del Portillo, I. Flores, A novel residential heating consumption characterisation approach at city level from available public data: Description and case study, Energy and Buildings 221 (2020) 110082, https://doi.org/10.1016/j.enbuild.2020.110082.

[34] Esri. (2024a). ArcGIS Pro v3.3. [Software]. https://pro.arcgis.com/en/pro-app/index-geonet-allcontent.html.

[35] Esri. (2024b). Working with the ArcGIS solution for 3D buildings. [Online]. https://www.esri.com/training/catalog/6410bcb84d750615175af71d/working-with-the-arcgis-solution-for-3d-basemaps/.

[36] Esri. (2023). Roof-Form extraction process, [Online]. https://solutions.arcgis.com/local-government/help/local-government-scenes/get-started/roof-form-extraction/.

[37] A.R. Suppa, A. Aliberti, M.C. Bottero, V. Corrado, Detecting window-to-wall ratio for urban-scale building simulations using deep learning with street view imagery and an automatic classification algorithm, Building Simulation 18 (8) (2025) 2175–2199, https://doi.org/10.1007/s12273-025-1301-3.

[38] Ultralytics., *YOLOv9 Documentation*, [Online]. https://docs.ultralytics.com/(2024).

[39] G. Kong, H. Fan, Enhanced facade parsing for street-level images using convolutional neural networks, IEEE Transactions on Geoscience and Remote Sensing 59 (12) (2021) 10519–10531, https://doi.org/10.1109/TGRS.2020.3035878.

[40] G. Sezen, M. Cakir, M.E. Atik, Z. Duran, Deep learning-based door and window detection from building façade, The International Archives of the Photogrammetry, Remote Sensing and Spatial Information Sciences 43 (2022) 315–320, https://doi.org/10.5194/isprs-archives-XLIII-B4-2022-315-2022.

[41] McNeel. (2024). Rhino v8 [Software]. https://www.rhino3d.com/.

[42] Ladybug Tools. (2024). Honeybee & Dragonfly. [Software]. https://www.ladybug.tools/.

[43] P. Felkel, S. Obrdrzalek, Straight skeleton implementation, in: *Proceedings of the 14th Spring Conference on Computer Graphics (SCCG)*, 1998, pp. 210–218.

[44] Y. Chen, T. Hong, M.A. Piette, Automatic generation and simulation of urban building energy models based on city datasets for city-scale building retrofit analysis, Applied Energy 205 (2017) 323–335, https://doi.org/10.1016/j.apenergy.2017.07.128.

[45] Y. Chen, T. Hong, Impacts of building geometry modeling methods on the simulation results of urban building energy models, Applied Energy 215 (2018) 717–735, https://doi.org/10.1016/j.apenergy.2018.02.073.

[46] A.R. Suppa , V. Corrado , Supporting the EU Mission "100-Climate Neutral Cities": Using Urban Building Energy Modeling for Zero-Emission Building Retrofit Scenarios at District Scale , Proceedings of Building Simulation 2023: 18th Conference of IBPSA (2023), 2946 - 2953. https://doi.org/10.26868/25222708.2023.1663.

[47] Italian National Unification Board (UNI) (2014). *Opaque envelope components of buildings - Thermo-physical parameters* (UNI/TR 11552:2014).

[48] Italian Republic. (2015). Inter-Ministerial Decree of 26 June 2015: application of energy performance calculation methodologies and definition of prescriptions and minimum requirements of buildings. [In Italian]. *Off. J. Ital. Repub. 2015, 162, 39*.

[49] Carsten Grobe Architecture Building Technology. (2020). Passive House criteria. [Online]. https://www.passivhaus.de/passivhaus/.

[50] L. Romero Rodríguez, E. Duminil, J.S. Ramos, U. Eicker, Assessment of the photovoltaic potential at urban level based on 3D city models: a case study and new methodological approach, Solar Energy 146 (2017) 264–275, https://doi.org/10.1016/j.solener.2017.02.043.

[51] Region of Veneto. (2024). Regional price list 2024. [Online]. https://www.regione.veneto.it/web/lavori-pubblici/prezzario-regionale.

[52] National Renewable Energy Lab (NREL). (2024). URBANopt Advanced Analytics Platform. [Software]. https://www.nrel.gov/buildings/urbanopt.html.

[53] United States Department of Energy (DoE). (2024). EnergyPlus. [Software]. https://energyplus.net/.

[54] Authority for Regulation of Energy Networks and Environment (ARERA). (2023). Annual report: state of services 2023. [Online]. https://www.arera.it/fileadmin/allegati/relaz_ann/24/RA24_vol1.pdf.

[55] Authority for Regulation of Energy Networks and Environment (ARERA). (2024). Update on minimum guaranteed price for 2024. [Online]. https://www.arera.it/comunicati-operatore/dettaglio/aggiornamento-dei-prezzi-minimi-garantiti-per-lanno-2024?ADMCMD_prev=LIVE.

[56] European Central Bank (ECB). (2024). The euro area inflation outlook: a scenario analysis. [Online]. https://www.ecb.europa.eu/press/key/date/2024/html/ecb.sp240830~ef0af8d7cc.en.html.

[57] European Central Bank (ECB). (2025). Economic Bulletin, Issue 2, 2025. [Online]. https://www.ecb.europa.eu/pub/pdf/ecbu/eb202502.en.pdf.

[58] S. Copiello, L. Gabrielli, P. Bonifaci, Evaluation of energy retrofit in buildings under conditions of uncertainty: the prominence of the discount rate, Energy 137 (2017) 104–117, https://doi.org/10.1016/j.energy.2017.06.159.

[59] P. Bragolusi, C. D'Alpaos, The valuation of buildings energy retrofitting: a multiple-criteria approach to reconcile cost-benefit trade-offs and energy savings,

Appl. Energy 310 (2022) 118431, https://doi.org/10.1016/j.apenergy.2021.118431.
[60] Region of Piedmont. (2024a). Regional price list 2024. [Online]. https://www.regione.piemonte.it/web/temi/protezione-civile-difesa-suolo-opere-pubbliche/prezzario-regione-piemonte-2024.
[61] R. Fedrizzi, C. Dipasquale, A. Bellini, M. Gustafsson, C. Bales, C., F. Ochs, G. Demerzentis, R. Nouvel, M. Cotrado. (2015). Inspire project: Performance of the studied systemic renovation packages – method.
[62] Dyaqua. (2023). Invisible solar – how it works & benefits.[Online]. https://www.invisiblesolar.it/EN/wp-content/uploads/2024/04/Brochure-Invisible-Solar-2023.11.21.pdf.
[63] Italian Superior Institute for Environmental Protection and Environmental Research (ISPRA), Italian greenhouse gas inventory 1990-2022: National Inventory Report 2024, ISPRA, Rome, 2024.
[64] Italian Revenue Agency. (2025). Update on deductions for interventions for the recovery of the building heritage and energy efficiency of buildings, and for interventions eligible for the Superbonus - Law No. 207 of December 30, 2024 (Budget Law 2025). [Online].https://www.agenziaentrate.gov.it/portale/documents/20143/8410825/CIRCOLARE+BONUS+EDILIZI+del+19+giugno+2025/8ee4bdaa-8080-d90c-989f-67947311e344.
[65] City of Turin. (2022). Registered population by gender and district 2022 data from 31/12/2022. [Online]. http://www.comune.torino.it/statistica/dati/2022/pdf/A1%20Pop%20per%20Sesso%20e%20Circ.pdf.
[66] City of Turin. (2023). *GIS database for City of Turin.* [Electronic database]. Used as per framework agreement between Turin and Politecnico di Torino pursuant to Art. 15 L. 241/1990.
[67] M. Noussan, Performance indicators of District heating Systems in Italy–Insights from a data analysis, Applied Thermal Engineering 134 (2018) 194–202, https://doi.org/10.1016/j.applthermaleng.2018.01.125.
[68] T. Charan, C. Mackey, A. Irani, B. Polly, S. Ray, K. Fleming, R. El Kontar, N. Moore, T. Elgindy, D. Cutler, M. Sadeghipour Roudsari, D. Goldwasser, Integration of Open-Source URBANopt and Dragonfly Energy Modeling Capabilities into Practitioner Workflows for District-Scale Planning and Design, Energies 14 (18) (2021) 5931, https://doi.org/10.3390/en14185931.
[69] X. Luo, T. Hong, Y. Tang, Modeling thermal interactions between buildings in an urban context, Energies 13 (9) (2020) 2382, https://doi.org/10.3390/en13092382.
[70] X. Xie, Z. Luo, S. Grimmond, T. Sun, W. Morrison, Impact of inter-building longwave radiative exchanges on building energy performance and indoor overheating, Building and Environment 209 (2022) 108628, https://doi.org/10.1016/j.buildenv.2021.108628.
[71] D. Kong, A. Cheshmehzangi, Z. Zhang, S. Pourroostaei Ardakani, T. Gu, Urban building energy modeling (UBEM): a systematic review of challenges and opportunities, Energy Efficiency 16 (69) (2023), https://doi.org/10.1007/s12053-023-10147-z.
[72] A. Banfi, M. Ferrando, P. Li, X. Shi, F. Causone, Integrating Occupant Behaviour into Urban-Building Energy Modelling: A Review of Current Practices and Challenges, Energies 17 (17) (2024) 4400, https://doi.org/10.3390/en17174400.
[73] Y. Zhang, X. Bai, F.P. Mills, J.C. Pezzey, Rethinking the role of occupant behavior in building energy performance: a review, Energy and Buildings 172 (2018) 279–294, https://doi.org/10.1016/j.enbuild.2018.05.017.
[74] Politecnico di Milano.(2025).URBEM—Urban Reference buildings for Energy Modelling. [Online]. https://www.urbem.polimi.it/.
[75] M. Ferrando, F. Causone, T. Hong, Y. Chen, Urban building energy modeling (UBEM) tools: A state-of-the-art review of bottom-up physics-based approaches, Sustainable Cities and Society 62 (2020) 102408, https://doi.org/10.1016/j.scs.2020.102408.
[76] J. Castagno, E. Atkins, Roof shape classification from LiDAR and satellite image data fusion using supervised learning, Sensors 18 (11) (2018) 3960, https://doi.org/10.3390/s18113960.
[77] Z. Qian, M. Chen, T. Zhong, F. Zhang, R. Zhu, Z. Zhang, K. Zhang, Z. Sun, G. Lü, Deep Roof Refiner: a detail-oriented deep learning network for refined delineation of roof structure lines using satellite imagery, International Journal of Applied Earth Observation and Geoinformation 107 (2022) 102680, https://doi.org/10.1016/j.jag.2022.102680.
[78] Enerdata. (2023). Carbon price forecast under the EU ETS.[Online]. https://www.enerdata.net/publications/executive-briefing/carbon-price-projections-eu-ets.html.
[79] Region of Piedmont. (2024). Special fees for landfilling of waste.[Online]. https://www.regione.piemonte.it/web/temi/tributi/altri-tributi/tributo-speciale-per-deposito-discarica-dei-rifiuti.
[80] European Committee for Standardization (CEN) (2019). *Energy Performance of Buildings. Ventilation for Buildings—Indoor Environmental Input Parameters for Design and Assessment of Energy Performance of Buildings Addressing Indoor Air Quality, Thermal Environment, Lighting and Acoustics* (EN 16798-1).